THE UNIVERSITY OF ALBERTA

THE EQUILIBRIUM PHASE PROPERTIES OF THE CARBONYL SULFIDE-PROPANE SYSTEM

by

ROGELIO DATUGAN MIRANDA

A THESIS

SUBMITTED TO THE FACULTY OF GRADUATE STUDIES AND RESEARCH
IN PARTIAL FULFILMENT OF THE REQUIREMENTS FOR THE DEGREE
OF MASTER OF SCIENCE IN CHEMICAL ENGINEERING

DEPARTMENT OF CHEMICAL ENGINEERING

EDMONTON, ALBERTA

FALL, 1974

To My Father

ABSTRACT

Equilibrium phase compositions and refractive indices were determined for the carbonyl sulfide-propane system using a windowed cell of variable volume. Measurements were made at temperatures of 20°, 60°, 100°, 140°, and 180°F and at a series of pressures ranging from the vapor pressure of propane to the vapor pressure of carbonyl sulfide at each temperature.

Pressure-composition diagrams for each isotherm showed an S-shaped configuration for both the saturated vapor and saturated liquid loci. Contrary to expectation, no azeotropes were encountered, although a tendency toward azeotropic behavior existed at the high concentration end for carbonyl sulfide.

The molar volumes of the co-existing phases were calculated from the measured refractive indices and equilibrium phase composition data using the Lorentz-Lorenz relationship. The pure component refractivities were assumed to be additive on a molar basis.

Early in the study, it became apparent that significant errors existed in the vapor pressures and critical properties reported for carbonyl sulfide. Accordingly, the vapor pressure and the refractive index of both liquid and vapor for pure carbonyl sulfide were measured. The new vapor pressure data are reported from 20°F to the critical temperature. The critical pressure was estimated to be 960 psia and the critical temperature to be 235°F. This compares

to earlier calculated values of 897 psia and 221°F respectively.

The experimental vapor pressure data for carbonyl sulfide were used to determine a value of 0.056 for Pitzer's accentric factor ω. This value, together with the critical properties, made it possible to estimate a value of 0.0044 for the k_{ij} interaction parameter for mixtures of propane and carbonyl sulfide.

The equilibrium data obtained at 100°F were used to estimate the constants needed in the Chueh-Prausnitz computer program developed for predicting the phase behavior of multicomponent systems. These constants were used to predict the data of this investigation at the remaining four isotherms. Close agreement between the experimental and predicted equilibrium ratios resulted. A thermodynamic consistency test was made on the data using the technique presented by Chueh, Muirbrook,and Prausnitz. The inconsistency ranged from 5.7 to 22.7 percent as the temperature changed from 20° to 180°F.

ACKNOWLEDGEMENTS

The author wishes to express his appreciation to Dr. D.B. Robinson for his encouragement and especially for his guidance in the supervision of this project.

The author gratefully acknowledges the valuable suggestions of Dr. H. Kalra, for his fruitful discussions during the course of the experiment and during the processing of the data. Thanks are due:

To Dr. D.Y. Peng for his helpful criticisms.

To Dr. P.R. Bishnoi for lending his integration subroutine.

To Mr. G.T. Walsh and his staff for their maintenance of the equipment and general support services provided by the workshop.

To Mr. D. Sutherland and his staff for their assistance in maintaining the instruments.

To Mr. D. Furnell for his assistance with the computer analysis.

To Mr. J.P. Moser for his assistance with laboratory analysis.

To Mr. Hans Rempis for his assistance in taking some of the experimental data.

To Mrs. Barbara Gallaiford for typing the manuscript.

The financial assistance from the National Research Council of Canada and from the Research Council of Alberta is gratefully acknowledged.

TABLE OF CONTENTS

LIST OF TABLES

LIST OF FIGURES

I - INTRODUCTION

Vapor-liquid equilibrium relationships are essential for the solution of many process engineering problems. In the design of distillation towers, absorbers, strippers, and other contacting equipment, a knowledge of the composition of the stream being treated and of the relative amounts of the co-existing phases under equilibrium conditions is needed.

The data required for these relationships are often determined experimentally. Over the years, a considerable amount of vapor-liquid equilibrium data have been accumulated by using a variety of techniques. Nevertheless, there are still a large number of industrially important systems whose equilibrium relationships have not yet been studied. Among these are the carbonyl sulfide-hydrocarbon systems.

Carbonyl sulfide is reported to be a common contaminant of refinery and synthesis gases[1]. It is believed to form during thermal or catalytic cracking and reforming operations and it exists in concentrations which vary from 10 to 20 ppm. Like other sulfur contaminants in hydrocarbon fluids, its presence is detrimental to the processing of the fluids or marketing of products derived from them[2]. Its vapor pressure characteristics and critical properties are very close to that of propane, thereby posing problems in the purification processes of the lower-boiling products[3]. Previous

studies on its separation showed that it is not satisfactorily removed by the conventional amine scrubbing processes employed by the industry for the removal of H_2S, mercaptans, and other sulfur bearing compounds. Instead, it reacts with amine solutions to form stable compounds by a complex re-arrangement so that the deactivated amine solutions can not be recovered by regeneration or revivification processes[1,2].

An experimental program to study the phase behaviour of the carbonyl sulfide-propane system was thus developed. The data obtained may then be used to estimate the binary interaction coefficient k_{ij} and other constants required for the analytical modelling of multicomponent phase behaviour according to the Chueh-Prausnitz[4] and the Soave-Redlich-Kwong[5] methods.

II - THEORY

A) Refraction

When light travels from one medium to another, it undergoes a change of velocity, and if the angle of incidence is not 90°, there will be a change in direction. This phenomenon is commonly known as refraction.

The law of refraction, widely referred to as Snell's law, has been attributed to W. Snell though other scholars[6] claimed that it was Descartes who made the first discovery in 1637. In any event, this law has been the basis for the determination of refractive indices.

Figure 1 demonstrates a ray diagram from which an expression for the refractive index may be deduced. From Snell's law, it follows that:

$$n_1 \sin\gamma = n_2 \sin\beta$$

$$n_2 \sin\beta = n_3 \sin\delta$$

$$n_3 = n_1 \sin\gamma / \sin\delta \qquad (1)$$

where n_1 is the refractive index of the ambient air, n_2 the refractive index of the glass window, and n_3 the refractive index of the fluid being measured. The angle δ is the prism angle and γ is the angle

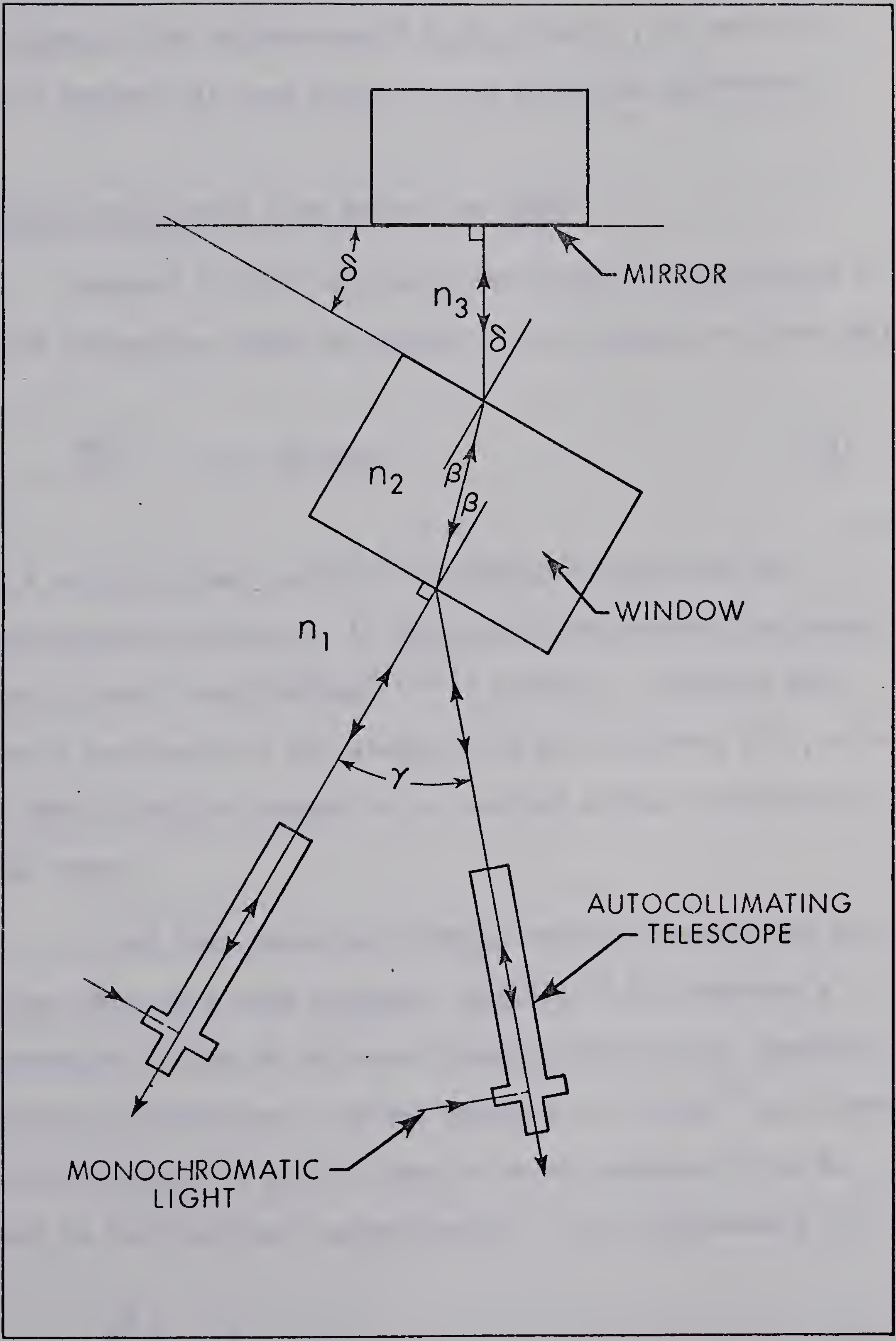

FIG. 1 SCHEMATIC REPRESENTATION OF THE ANGLE MEASUREMENT INVOLVED IN THE DETERMINATION OF THE REFRACTIVE INDEX

[illegible]

measured by autocollimation. For a light source of given wavelength, n_1 is known, δ can be measured if $n_3=n_1$, that is, if the cell contains ambient air, and hence, n_3 can easily be determined.

B) Density Measurement From Refractive Index

Newton[7] in 1704 introduced the concept of refraction in terms of refractive index and density. His formulation shows that:

$$\frac{n-1}{d} = r_1 = \text{constant} \tag{2}$$

About a century later, Laplace[8] in 1806 postulated that the proportionality constant r_1 is invariant with pressure and temperature. Later investigations[9,10,11] however , indicated that Laplace's conclusion is not always valid but variation of r_1 is so small that it may be assumed to be constant without introducing serious error.

Since then, numerous formulae relating density and refractive index have been proposed. Besserer[12] has reported a comprehensive review of the more relevant refractivity formulae. Among these correlations, the one proposed by Lorentz[13] and Lorenz[14] is widely accepted in optical physics mainly because it can be related to the electronic polarizability. The relationship is:

$$\frac{n^2-1}{n^2+2} \quad \frac{M}{\rho} = R_{LL} \tag{3}$$

where R_{LL} is the molar refractivity. Batsanov[14] outlined the derivation of this formula from electromagnetic theory.

The relationship of refractive index and density was originally tested on pure substances. Subsequently, scientists established the effect of composition on the refractivity of mixtures. The work of Biot and Arago[16,17]; Smith, Engel, and Wilson[18]; Young and Finn[19]; Keilich[20]; and Bloom and Rhodes[21] showed that pure component refractivities are nearly additive in their molar ratios to give refractivities of mixtures. The deviations from this assumption are small (about 1 to 2%) and within the accuracy of most experimental techniques. Thus, the assumption that mixture refractivities can be expressed by a molar sum of the pure component refractivities is justifiable.

C) Vapor-Liquid Equilibrium

Generally speaking, a system is said to exist in equilibrium if no change in the condition of the system occurs with time. These changes are brought about by resistances and by driving forces. Some of these forces are attributed to pressure and/or temperature gradients and chemical potentials.

In reality however, a true state of equilibrium is probably never reached. There is a continual variation in our surroundings caused by resistances which have a tendency to diminish with time.

Nevertheless, as equilibrium is approached the rates of change become very small so as to become immeasurable by available means. For practical purposes this state might be considered as a state of equilibrium. In many engineering problems the assumption of equilibrium is justified when the results assuming a state of equilibrium are of satisfactory accuracy[22].

The condition of equilibrium can be expressed in terms of thermodynamic variables. Combining the first and second laws of thermodynamics, it can be shown that:

$$(d\,U_{system} + Pd\,V_{system} - Td\,S_{system}) = 0 \qquad (4)$$

Various restraints may be put on the above expression to produce alternative conditions; for example:

$$(d\,U_{system})_{S_{system},\ V_{system}} = 0 \qquad (5)$$

Alternatively, other pairs of properties may be held constant. The most useful result comes from fixing T and P. In so doing,

$$d(U_{system} + P\,V_{system} - TS_{system})_{T,P} = 0 \qquad (6)$$

The term inside the bracket is commonly known as the Gibbs Free Energy (G). Therefore, for a system to be in equilibrium:

$$d(G_{system})_{T,P} = 0 \qquad (7)$$

The application of this criterion to a multiphase closed system gives the generalised condition of phase equilibrium:

$$\mu_i{}' = \mu_i{}'' = \mu_i{}''' \; . \; . \; . \; . \qquad (8)$$

where μ_i's are the chemical potentials of i in each phase. Alternatively, equation (8) can be transformed to the more convenient relation for the prediction of multi-phase, multicomponent equilibria:

$$\hat{f}_i{}' = \hat{f}_i{}'' = \hat{f}_i{}''' \; . \; . \; . \; . \qquad (9)$$

where $\hat{f}_i$'s are the fugacities of i in each phase. Restricting our phases to liquid and vapor, equation (9) would result to the fundamental criteria for vapor-liquid equilibrium:

$$\hat{f}_i{}^L = \hat{f}_i{}^V \quad (i=1,m) \qquad (10)$$

The general vapor-liquid equilibrium problem involves a multicomponent system of m components for which the independent variables are T and P, $m-1$ liquid mole fractions, and $m-1$ vapor mole fractions. Thus, there are 2m independent variables. Application

of the phase rule shows that exactly m of these variables must be fixed; while the remaining m variables can be determined by simultaneous solution of m equilibrium relations from equation (10). Specifying either the liquid-phase compositions or the vapor-phase compositions and either T or P would amount to fixing m independent variables. Hence, the remaining m variables are subject to calculation.

Fugacity is expressed for each phase as:

$$\text{Liquid:} \quad \hat{f}_i^{\,L} = \hat{\phi}_i^{\,L} \; x_i \; P \tag{11}$$

$$\text{Vapor:} \quad \hat{f}_i^{\,V} = \hat{\phi}_i^{\,V} \; y_i \; P \tag{12}$$

At equilibrium:

$$x_i \; \hat{\phi}_i^{\,L} \; P = y_i \; \hat{\phi}_i^{\,V} \; P \tag{13}$$

This introduces the composition x_i and y_i into the equilibrium relation, but neither are explicit because the $\hat{\phi}_i$'s are functions of composition. In addition, $\hat{\phi}_i$'s are functions of T and P. Thus, equation (13) represents m relationships connecting T, P, x_i's and y_i's. For computer solution of this equation it is essential that the $\hat{\phi}_i$'s be expressed analytically as functions of T, P, and composition. This requires an equation of state which accurately represents the

volumetric properties of both the vapor and liquid phases throughout the range of pressures, temperatures, and compositions of interest.

Most of the computer calculations[4,23] on vapor-liquid equilibrium use the two-parameter Redlich-Kwong equation of state in determining the vapor phase fugacity coefficient. This is probably so because the constants of the equation can be evaluated from the critical temperature and pressure for the pure components constituting the system, and the binary interaction coefficients k_{ij} for multicomponent systems. The eight-parameter Benedict-Webb-Rubin (BWR) equation of state[24] is also widely employed, but a large amount of volumetric data is required to evaluate the constants. Such constants are available for a relatively few substances[25,26,27,28].

Another approach in solving equation (13) is by using the concept of activity coefficients in the liquid phase. Based on Raoult's law and the concept of fugacity, the fugacity of a component in a liquid phase is given by:

$$\hat{f}_i^L = \gamma_i \, x_i f_i^0 \tag{14}$$

where γ_i is the activity coefficient and f_i^0 the standard state fugacity coefficient of the substance. Retaining the same relation of $\hat{f}_i^V$, equation (13) will become:

$$\gamma_i \, x_i \, f_i^0 = \hat{\phi}_i \, y_i \, P \tag{15}$$

The purpose of the activity coefficient, γ_i is to relate the unknown fugacity to its standard state value, f_i^0, which is the fugacity of pure i at the temperature and pressure of the system.

The activity coefficient γ_i is related to the Gibbs function as follows:

$$\frac{G^E}{RT} = \sum (x_i \ln \gamma_i) \tag{16}$$

or,

$$\ln \gamma_i = \frac{G^E}{RT} - \sum_{K \neq i} x_K \left[\frac{\partial (G^E/RT)}{\partial x_K} \right]_{T,\ P,\ x_r} \tag{17}$$

$r \neq i, K$

Thus, for a given T and P and composition, γ_i can be evaluated if G^E is known as a function of composition.

Activity coefficients can also be calculated from experimental vapor-liquid equilibrium data by the use of the following equation:

$$\ln \gamma_i = \ln \frac{y_i P}{x_i} + \ln \hat{\phi}_i - \ln f_i^0 \tag{18}$$

To be of greater use, these coefficients are often correlated by equations, the best examples being the van Laar equations and the

Margules equations.

In summing up the analytical solution to a vapor-liquid equilibrium, it is sufficient to say that given a suitable equation of state with known constants for the vapor phase, data for the standard states, and an appropriate relation of activity coefficients in the liquid phase, the unknown variables can be determined.

III - PREVIOUS WORK

A) Carbonyl Sulfide (COS)

The existence of carbonyl sulfide was not confirmed until 1867 when Than[29] reported it by the reaction of carbon monoxide and sulfur vapors. Since then, numerous investigators have prepared it in a variety of ways. A comprehensive review of these methods and the chemistry involved has been presented by Ferm[3].

(i) Vapor Pressure

Earlier studies on the vapor pressure of carbonyl sulfide were made by Ilosvay[30], Hempel[31], and Stock and Kuss[32]. These investigations however, were conducted only for a limited number of temperatures. The International Critical Tables[33] report the work of Ilosvay but some contradictions in the reported data were observed. In 1936, Kemp and Giauque[34] measured COS vapor pressures from 161.8 K to 223.8 K. The data were fitted to the following equation:

$$\log_{10}(P) = -(1318.260/T) + 10.15309 - 0.0147784T + 0.000018838T^2 \qquad (19)$$

where P is the absolute pressure in cm. Hg., and T is the absolute temperature in K. Later, Honig and Hook[35] developed another equation

to fit these vapor pressure observations. The Matheson Gas Products Company in their latest publication[36] on COS properties presented a vapor pressure diagram based on the equation of Kemp and Giauque, but extended its use to temperatures well beyond the range for which it was developed.

(ii) Density

The density of saturated liquid COS at -87°C was measured to be 1.24 g/cc by Stock and Kuss[32] as compared to a value of 1.30 g/cc suggested by Pearson, Robinson, and Trotter[37] at the same conditions. Orthobaric densities for liquid COS were obtained by Partington and Neville[38] from -99.5°C to 100.9°C, however, their data showed a disagreement of up to 4% when compared to the work of Stock and Kuss[32] and Pearson et al[37]. The only vapor density measurement for COS was reported by Kemp and Giauque[34]. At 25°C and atmospheric pressure, the value was reported to be 2.4849 g/cc.

(iii) Critical Properties

The critical temperature of COS was reported to be 105°C by Ilosvay[30] and Hempel[31], but it was measured to be 102.2°C by Partington and Neville[38]. From the vapor pressure data of Stock and Kuss, Kobe and Lynn[39] estimated the critical pressure to be 61 atm. A critical pressure estimation made by Lydersen[40], however, indicated a value of 65 atm.

(iv) Refractive Index

The refractive index of liquid COS was measured by Francis[41] and Wong and Anderson[42]; the latter reported the molar refractivity to be 11.29 cc/g.-mole.

(v) Other Properties

The phase diagram for COS was presented by Babb[43], and the solubility of COS with some organic solvents were measured by Kir'yanova and Pinsker[44].

In addition to vapor pressure and vapor density measurements, Kemp and Giauque[34] also determined its melting point, boiling point, heat capacities, and heats of fusion and vaporization. Other thermodynamic properties for COS have been calculated by Kobe and Lynn[39], Kobe and Long[45], McBride and Gordon[46], Zandler, Watson, and Eyring[47], and Cross[48].

Because COS occurs as a contaminant in many refinery gases, its corrosive properties are of interest. Nelson, Veal, and Heinrich[49] verified that COS does not produce a tarnished strip in their copper corrosion test. However, Freise[50] discovered that COS is corrosive toward concrete. Except for these findings, information is not available on the action of COS towards other metals.

B) Propane

Information on the critical properties, vapor pressure

characteristics, density and other thermodynamic properties of propane have been reported by many authors[51-56]. Its behaviour with other hydrocarbons and nonhydrocarbons is extensively reported in the literature[57-75]. A detailed review on this work will not be included here for it is beyond the scope of this study.

C) Carbonyl Sulfide-Propane Binary

No information is available on this system. And as mentioned earlier, no studies have been conducted on the vapor-liquid equilibrium of carbonyl sulfide with other substances.

IV - THE EXPERIMENTAL STUDY

The objective of the experimental program was to obtain pressure-composition diagrams for the carbonyl sulfide-propane system simultaneously with the co-existing phase densities.

The densities of the co-existing phases were calculated from refractive index measurements which were taken twice for each phase. Vapor and liquid phase compositions were analyzed using a gas chromatograph. Two samples of each phase were analyzed three times and the average of the six analyses was accepted.

A) Experimental Apparatus

A detailed description of the equipment design has been presented in earlier publications[76,77]. Although no significant modification was made to the original equipment, it is considered desirable to mention some of the more pertinent features here.

A schematic diagram of the apparatus and its associated equipment is shown in Figure 2 and the essential features of the cell design are shown in Figure 3. The cell, machined from 4 inch diameter type 316 stainless steel, consists of three parts, two cylinder piston end sections and a central windowed section. The three sections are bolted together with high pressure seals between them made by flattened Teflon O-rings. On assembly, it has an over-

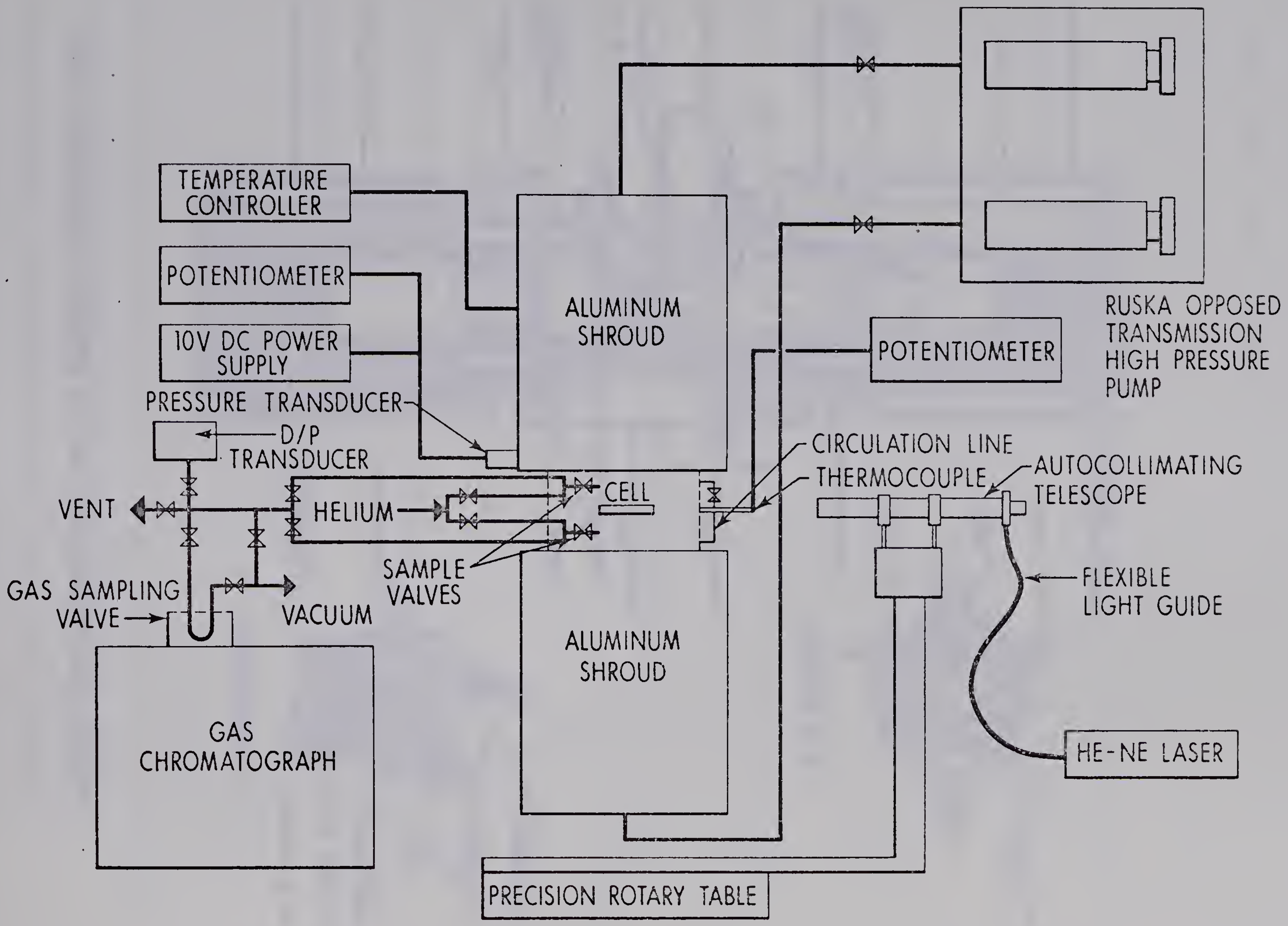

FIG. 2 SCHEMATIC DIAGRAM OF THE CELL AND ITS ASSOCIATED EQUIPMENT

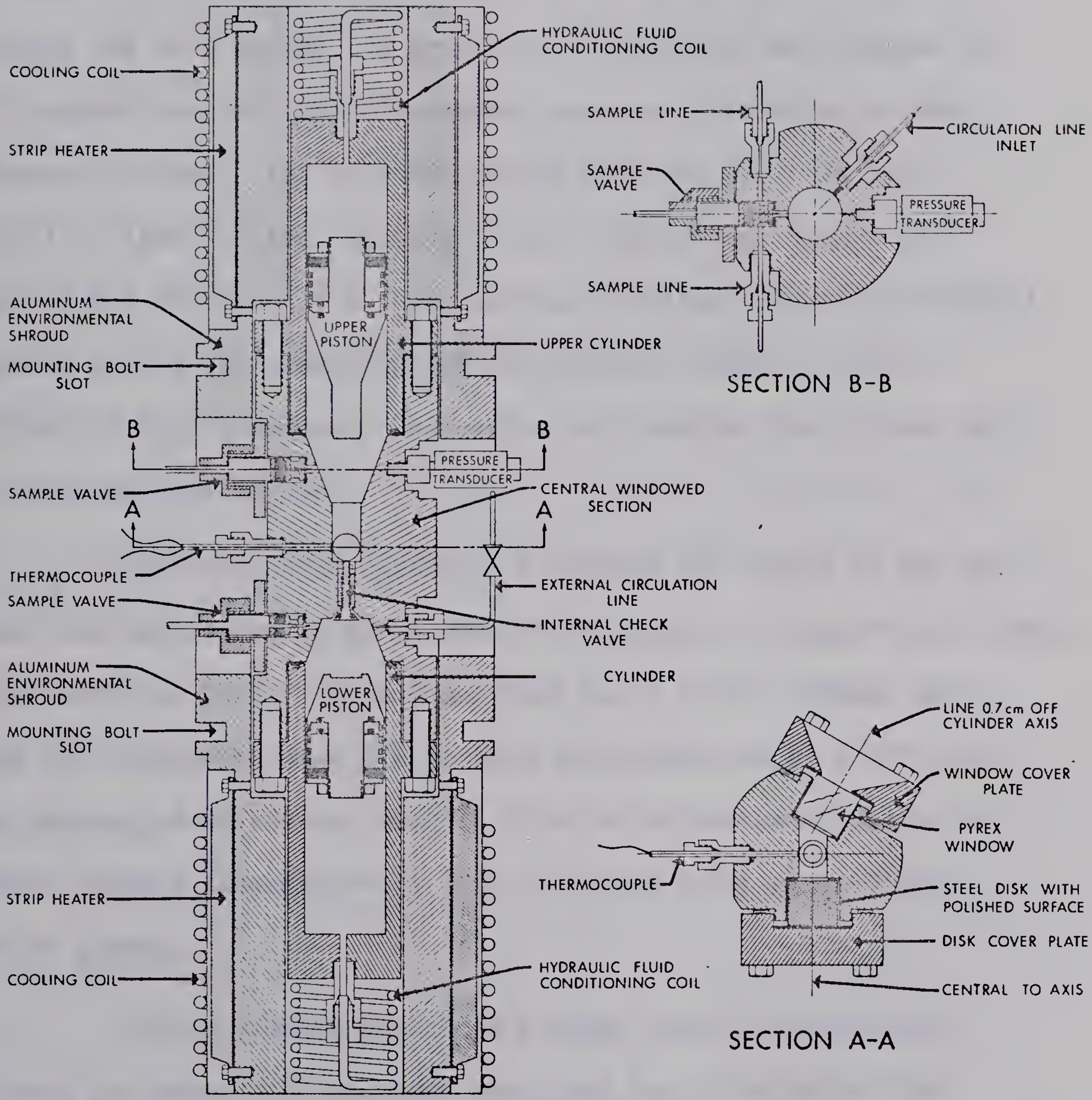

FIG. 3 ESSENTIAL FEATURES OF THE EQUILIBRIUM CELL DESIGN

all length of 19 inches. Each piston has a 4 inch travel and is confined to its respective cylinder. A low viscosity silicone oil is employed as the hydraulic fluid. This provides a means for varying the cell volume and pressure. The piston seal between the oil chamber and the central windowed section is effected by four neoprene-O-rings. The original design made use of a 316 type stainless steel piston. However, later indications showed that wearing out of the cell's inner surface resulted from metal to metal contact during the travelling of the pistons, especially when working at high pressure. To resolve the problem, the pistons were re-machined from Teflon.

The horizontal section A-A through the center of the cell shows how the window, a pyrex disk 1-1/8 inches in diameter and 1 inch thick with its faces flat and parallel to $\pm 4 \times 10^{-5}$ inches, and a type 316 stainless steel mirror form the boundaries of a 30° prism. The window and mirror are held in place by bolted cover plates and sealed against lapped surface with 1/16 inch thick glass-filled Teflon gaskets.

The horizontal section B-B shows one of the sampling valves, the pressure transducer port, and the circulation line outlet. The sampling valves are internally mounted Circle Seal MV-92 micro-metering valves with provision made for flushing out and evacuation of the low pressure sampling line. The circulation system used to attain equilibrium consists of an internal check

valve in the central section and an external 1/8 diameter stainless steel line with a shut-off valve.

Cell Temperature Control

The temperature of the cell is maintained by two 7 inch diameter aluminum environmental control shrouds which are placed over the end of the cell as shown in Figure 2. Each shroud includes four 150 watt strip heaters and a 20 foot cooling coil. A Thermac proportional plus integral controller operates the heaters in both shrouds and controls the cell temperature to within ± 0.1°F of the setpoint.

When working at isotherms below ambient temperature, the cell is cooled by circulating ethylene glycol-water mixture refrigerated by freon-12.

The cell is capable of operating from 2°F to 250°F in normal ambient room conditions.

Optical System

A telescope (Gaertner M523 aperture 28 mm., f.l. 250 mm.) with an Abbe-Lamont autocollimating eyepiece (Gaertner 1372) is mounted on a 10 inch diameter precision rotary table (Karl Kneise RTHP-10) with a two second vernier handwheel and a maximum table error of 10 seconds in 360 degree of rotation. The table is centered under a point on the front surface of the pyrex cell window. Monochromatic light at a wavelength of 6328 Å is provided by a Helium-

Neon gas laser and is transmitted to the eyepiece by a glass fiber light guide.

The refraction angle γ shown in Figure 1 is measured by autocollimation. The measured angles have a repeatability of ±4 seconds and a table error of ±2 seconds over the measured range. The refractometer has an over-all possible error of $\pm 6 \times 10^{-5}$ in the refractive index and a possible range of 1.0 to 1.7.

Operational Procedure

The conventional way of working with binary systems involves charging the heavier component first following by adding the lighter component. In this study, the carbonyl sulfide (the lighter component)used has a maximum purity of 97.6 mole percent in the liquid phase and as such had to be purified before any binary data could be taken. The bulk of the impurities consisted of lighter substances which could be effectively removed by fractional distillation. For convenience, the carbonyl sulfide was charged first and was fractionally distilled inside the cell. Propane was subsequently added to make up the pressure to the desired level. This was achieved by boosting the feeding pressure of propane in the cylinder with a hot water bath. A propane cylinder pressure of at least 65 psia greater than the cell pressure was considered adequate to prevent contamination of the cylinder with the contents of the cell.

The two pistons in the end sections were hydraulically driven by a motorized dual cylinder high pressure pump with an opposed transmission (Ruska Model 2248 WII). This allowed both

pistons to be moved simultaneously up or down maintaining the volume between them constant. The possible working volume ranges from 10 cc to 174 cc.

Mixing and equilibration were attained by running the pistons up and down simultaneously. On the upstroke, the internal check valve closes and the fluid is forced through the external circulation line and sprayed into the upper cylinder through a nozzle. On the downstroke, the circulation line valve is closed and the fluid passes through the internal check valve. Five to ten cycles were usually sufficient to attain equilibrium.

The point at which equilibrium is achieved can be verified by observing the line images in both phases through the autocollimating telescope. These images are very sensitive to composition and temperature fluctuations and become stable when the equilibrium state is attained. The angle γ was measured by observing the location of the line images obtained through normal light incidence on the glass window and the mirror.

The temperature was measured with an iron-constantan thermocouple sheathed in 316 stainless steel with its tip exposed to the fluid in the prism. The pressure was measured with a 3000 psi 316 stainless steel bourdon tube Heise Gauge or a 1500 psi strain gauge transducer (Consolidated Electronics).

Samples of liquid or vapor were expanded to a pressure of

0.2 atmospheres through a micro-metering valve into the evacuated line connected to the gas chromatograph gas sampling valve. The pressure in the sampling line was measured with a differential pressure transducer. Two samples of each phase were taken and triplicate chromatographs were run on each sample. The average size of each sample corresponds to a 0.2 percent depletion of an average load. The pressure drop associated with the taking of a sample was always less than 3 psia. For each point the six analyses, three from each of two samples, were generally repeatable to within 0.2 mole percent and their accuracy is probably 0.3 percent. The pressure is believed known to ±3 psia and the temperature to ±0.1°F.

The gas chromatograph used was a Hewlett-Packard Model 700 machine equipped with a thermal conductivity cell detector. The signal from the gas chromatograph was detected by an on-line IBM-1800 Computer and peak integrations were obtained by using available software. The results of the analysis were printed out on a teletype.

Operating conditions for the gas chromatograph were as follows:

Column	:	Porapak QS
Column Size	:	1/8" dia. x 6'
Carrier Gas	:	Helium at 20 c.c./min.

Column Temperature : 75°C
Filament Current : 180 ma.
Detector Temperature : 200°C
Area Integration : Electronic

The conditions given above were experimentally determined to be optimum considering separation and time of analysis. The gas chromatograph was calibrated using the pure components only and the response was found to be linear for the range of the sample loop pressures encountered. The resulting calibration curve is shown in Figure 20. The response factor of propane relative to carbonyl sulfide was calculated to be 0.995.

B) Materials

Matheson instrument grade carbonyl sulfide was used. Chromatographic analysis indicated it to contain 97.6 mole percent COS in the liquid phase and 84.1 mole percent COS in the gas phase, the major impurity being carbon dioxide. Because of the impurity, further purification was necessary, and it was carried out in two stages. Liquid COS was drawn into a 500 ml. stainless steel sample bomb (Hoke DS 5-52), connected to a 3000 psi stainless steel Heise gauge. After isolation from the main cylinder the contents of the sample bomb were cooled by liquid nitrogen. When the gauge registered a pressure of about 10 psi, the supply of nitrogen was shut

off, and the sample was fractionally distilled by venting the vapor phase. To minimize the loss of COS, the fractionation was stopped when the pressure reached about 120 psig. This step was carried out four to five times. Analysis of the vapor phase after the final fractionation indicated it to contain approximately 98.5 mole percent COS. Further fractionation made very small improvement in the purity.

The second stage in the purification was done inside the equilibrium cell. A liquid sample of about 120 cc, purified from the first stage, was charged to the cell. Since the cell was equipped with a micro-metering valve, the vapor phase could be bled off slowly. The pistons in the end sections were adjusted occasionally in such a manner that the interface of the liquid and vapor was always visible in the window, and vaporization of the liquid could be kept to a minimum. When about 40 cc of liquid were left, the vapor phase was analyzed. It was found to contain about 99.5 mole percent COS. Subsequent bleeding off had a negligible effect on the purity. The COS used in the study was thus of a 99.5 percent minimum purity. The second stage purification generally took about 4 to 5 hours.

The propane used was Matheson Instrument grade. It was analyzed and found to contain better than 99.9 mole percent in the liquid phase and 98.0 mole percent in the vapor phase, the major impurities being methane and nitrogen. Due to this purity the liquid phase was used in the study.

V - EXPERIMENTAL RESULTS

The phase behaviour of the carbonyl sulfide-propane binary system was studied at 20°, 60°, 100°, 140°, and 180°F, with pressures ranging from the vapor pressure of propane to the vapor pressure of carbonyl sulfide. An average of 10 points, generally equally spaced in pressure between pure propane and pure COS vapor pressures were taken for each isotherm.

The equilibrium phase compositions for each of the five isotherms were analyzed. The refractive indices of the co-existing phases were measured and the molar volumes calculated using a molar averaged Lorentz-Lorenz refractivity. The refractive indices of pure propane and pure COS were also measured for each of the isotherms from saturation pressure up to about 1000 psia. For COS, the refractive index measurement was extended to 230°F. This provided sufficient data to plot saturation pressure versus refractive index, from which an estimate of the critical pressure could be obtained. The vapor pressure curve for COS was plotted from 20°F to the estimated critical point.

A) Refractive Indices of Carbonyl Sulfide and Propane

Experimentally determined refractive indices of the compressed liquid for pure COS and propane are plotted with pressure,

and are presented in Figures 4 and 5, respectively. These data are also tabulated in Tables 1 and 2 in the Appendix.

B) Refractive Indices of Carbonyl Sulfide at Saturated Conditions

Table 3 in the Appendix shows the experimentally measured refractive indices of saturated carbonyl sulfide from 20°F to 230°F. Figure 6 gives a plot of the saturation pressure versus the refractive index for the vapor and the liquid.

The critical point estimated from Figure 6 is plotted along with the vapor pressure data obtained for carbonyl sulfide in Figure 7.

C) Co-existing Phase Properties of the Carbonyl Sulfide-Propane System

Figures 8, 9, 10, 11, and 12 show the plots of the experimentally determined phase compositions with pressure. The data indicate the distinct S-shaped configuration of the P-x diagrams.

Plots of the measured refractive indices are shown in Figures 13 and 14. The molar refractivities of propane were calculated using the volumetric data predicted by the BWR equation with improved coefficients[28], and the measured refractive indices. For COS, the necessary volumetric data were interpolated from those values reported by Partington and Neville[38]. The molar volumes of the co-existing phases were calculated using a molar average Lorentz-Lorenz re-

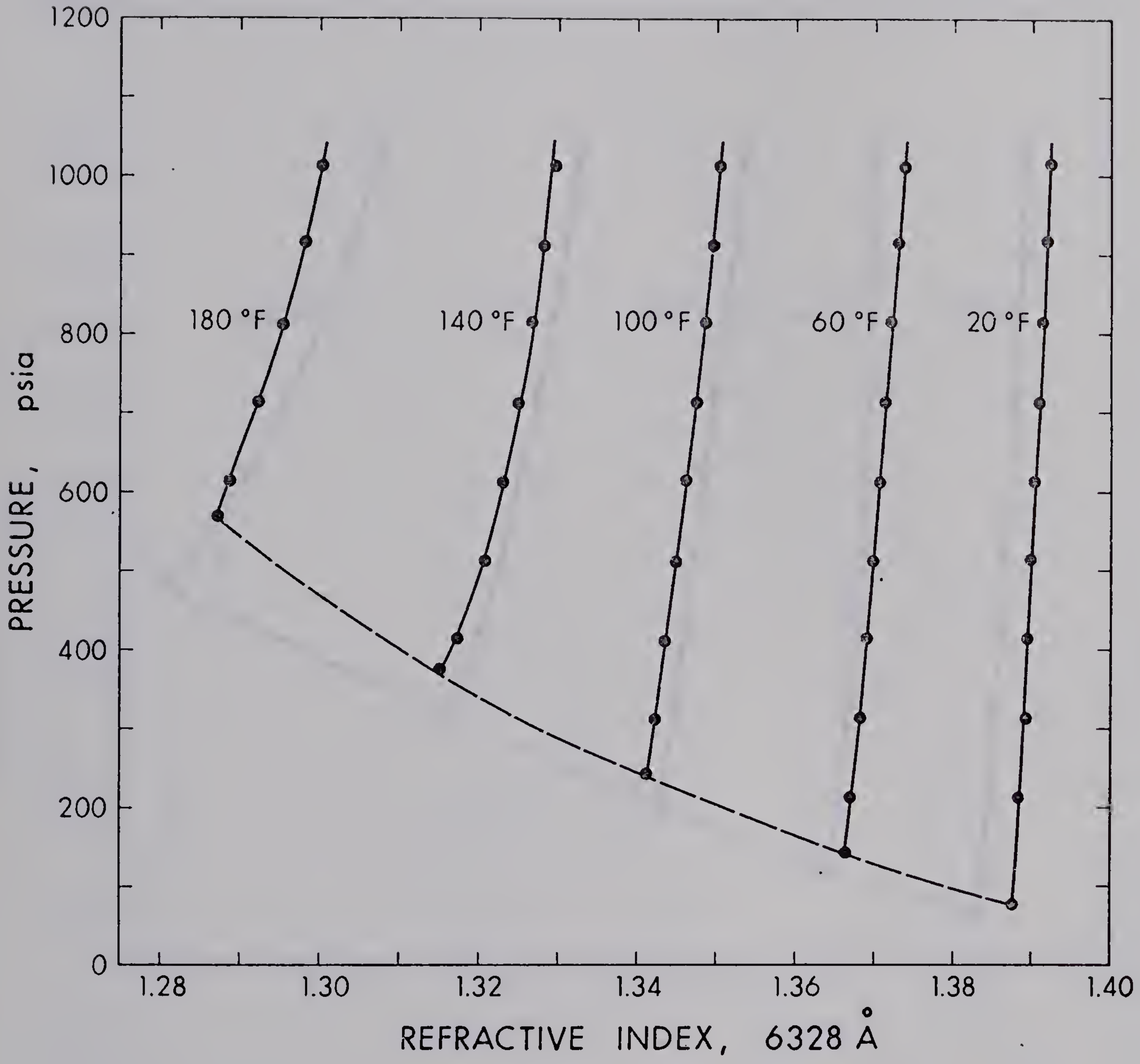

FIG. 4 EFFECT OF PRESSURE AND TEMPERATURE ON THE REFRACTIVE INDEX OF CARBONYL SULFIDE

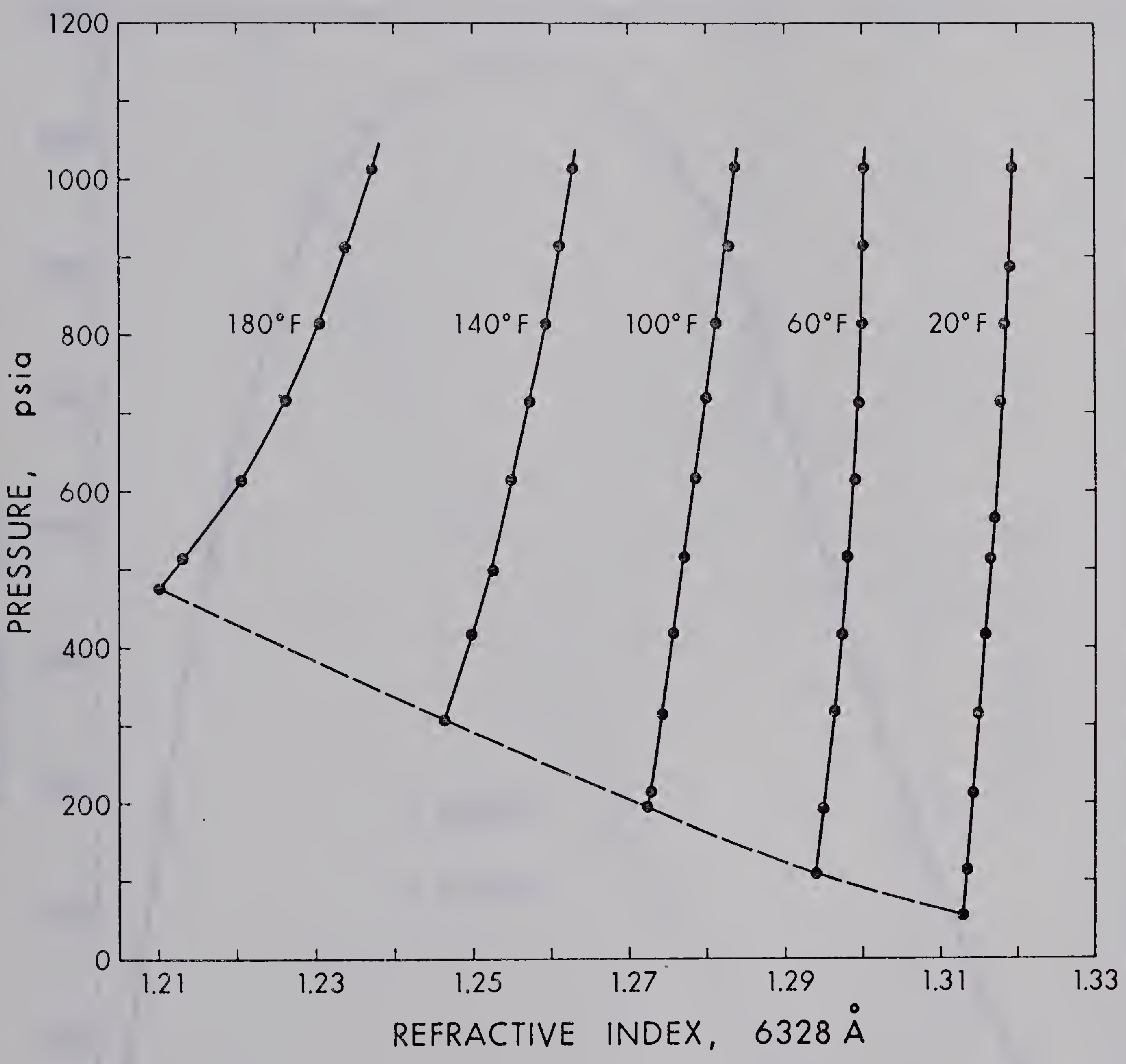

FIG. 5 EFFECT OF PRESSURE AND TEMPERATURE ON THE REFRACTIVE INDEX OF PROPANE

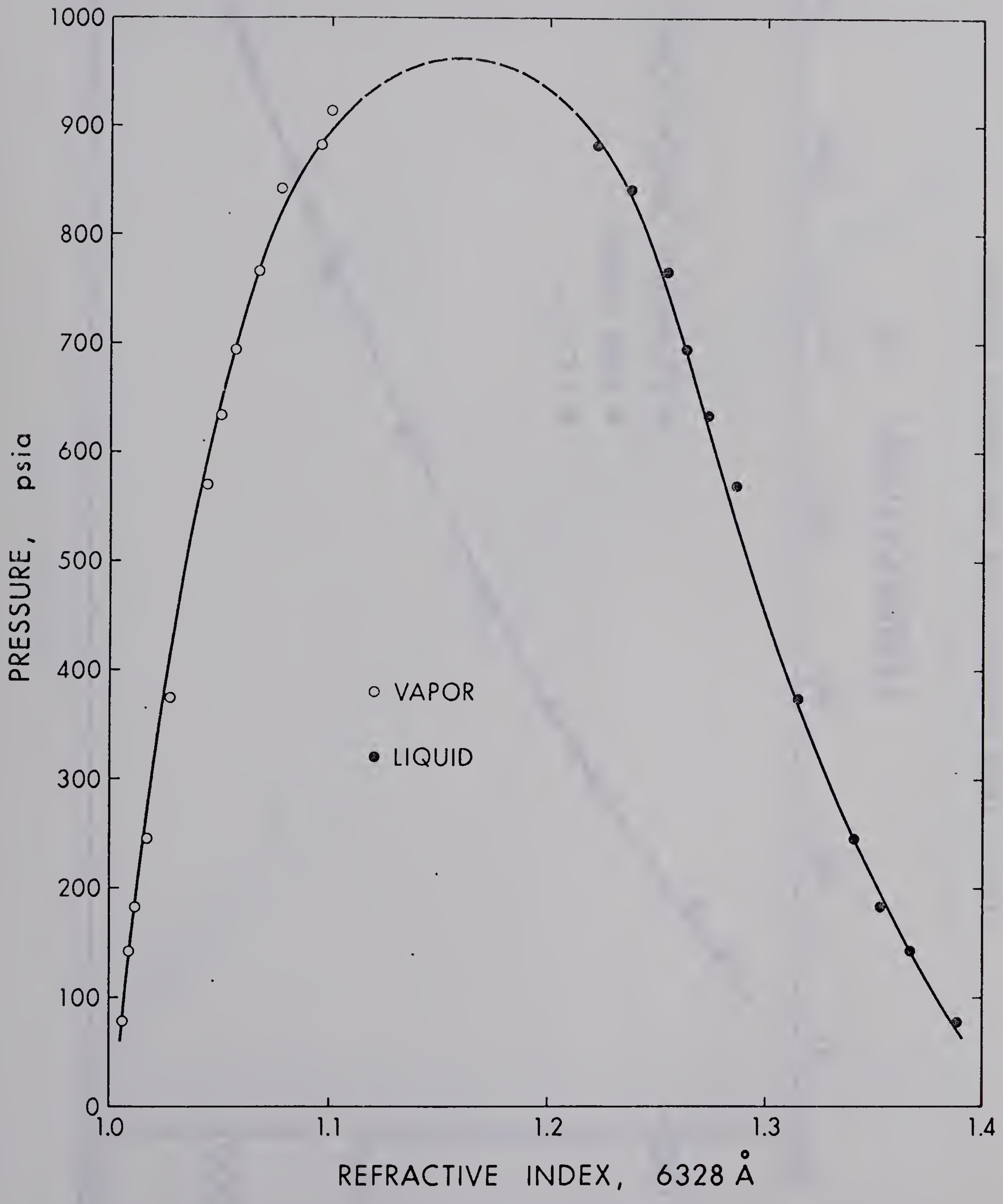

FIG. 6 PRESSURE VS. REFRACTIVE INDEX PLOT OF CARBONYL SULFIDE AT SATURATED CONDITIONS FOR CRITICAL POINT DETERMINATION

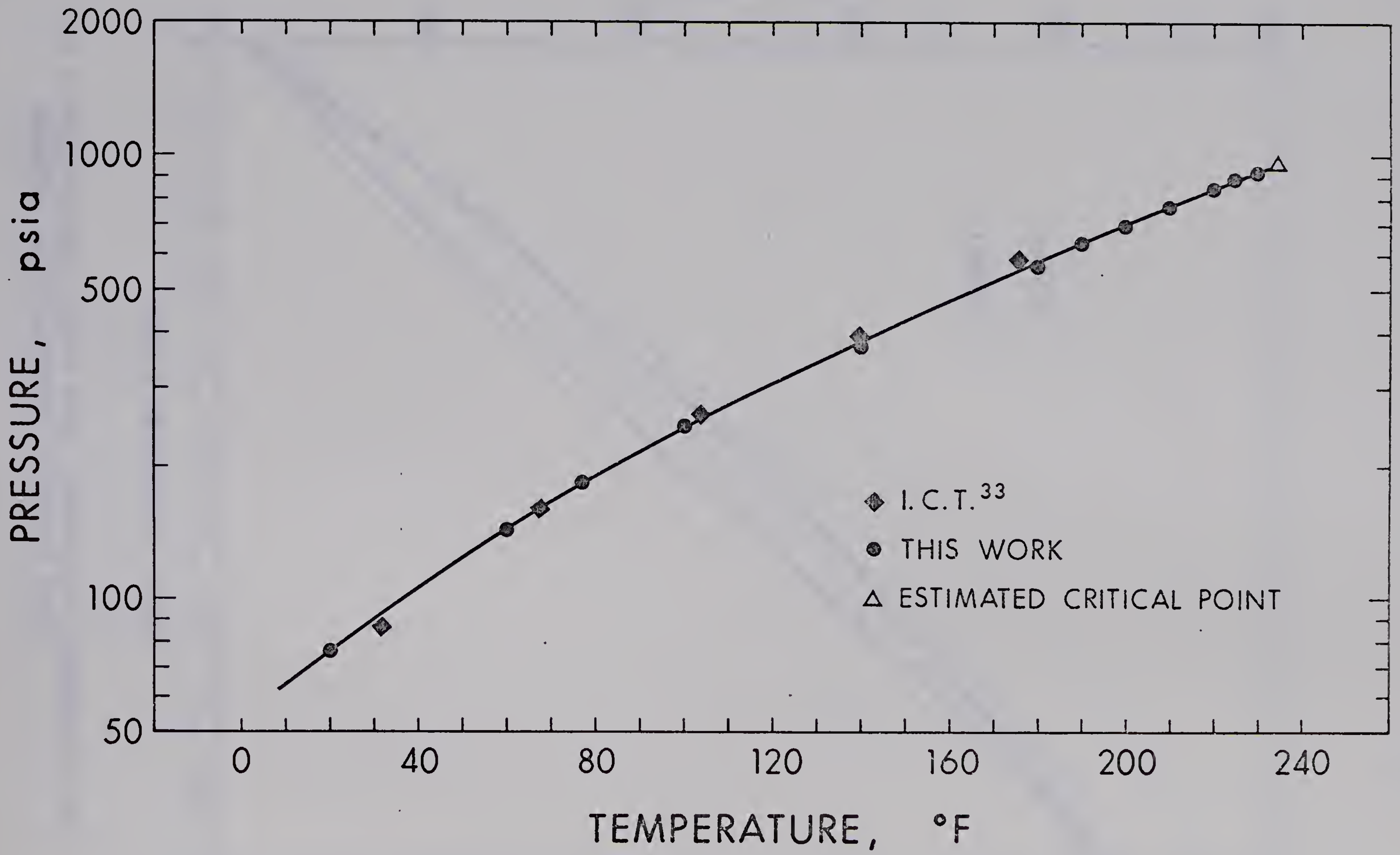

FIG. 7 VAPOR PRESSURE CURVE FOR CARBONYL SULFIDE

[illegible]

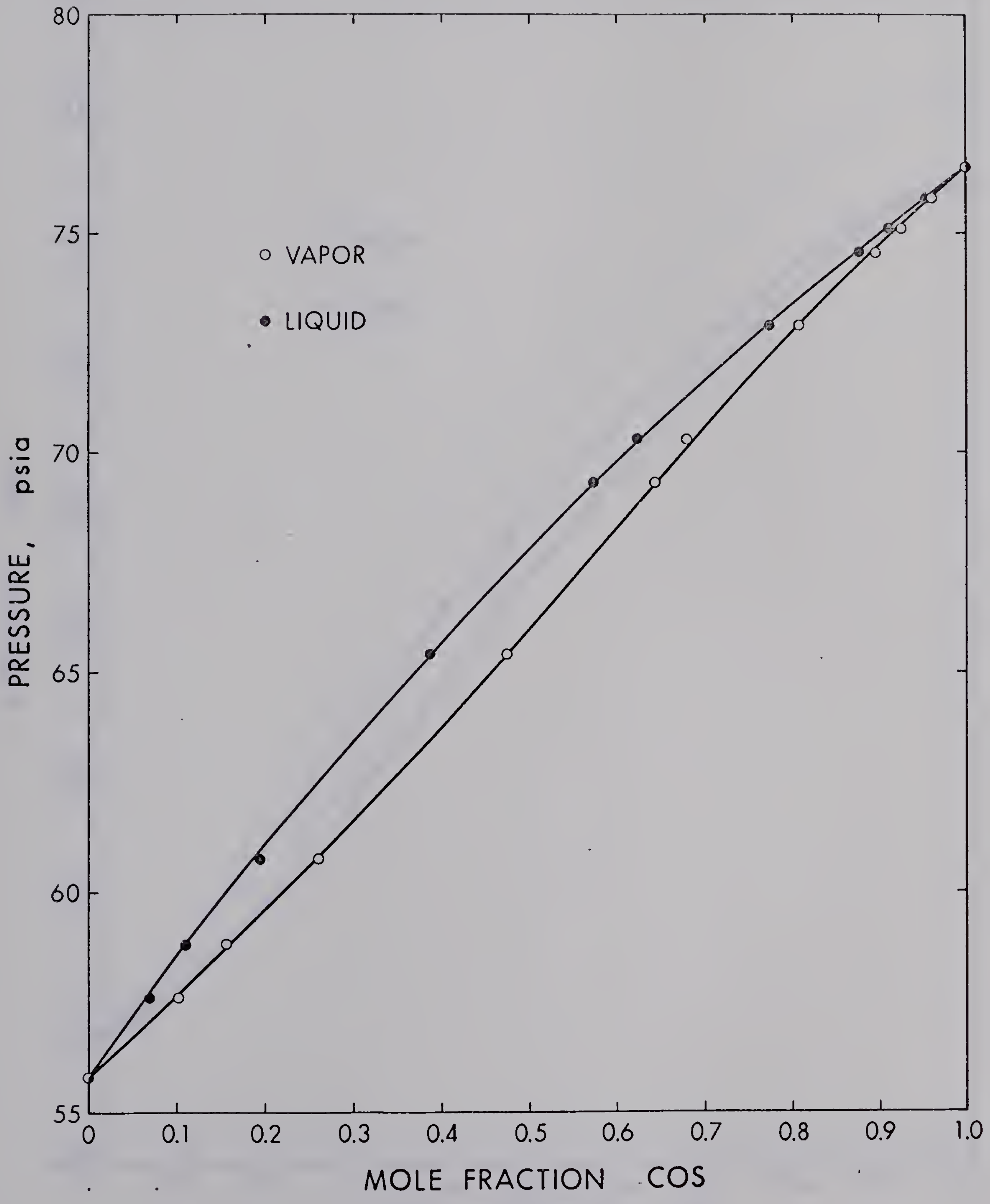

FIG. 8 PRESSURE-EQUILIBRIUM PHASE COMPOSITION DIAGRAM FOR THE CARBONYL SULFIDE-PROPANE SYSTEM AT 20°F

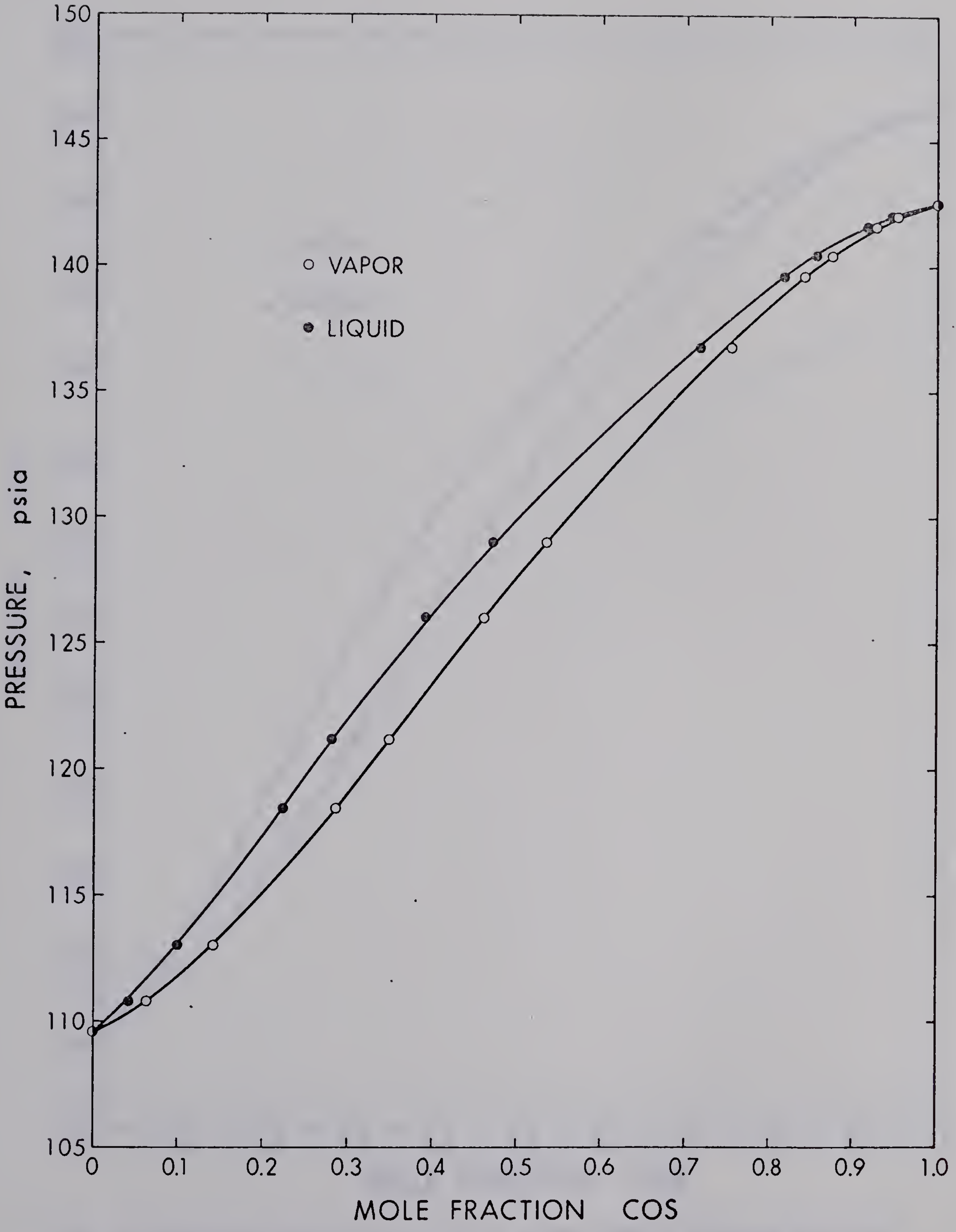

FIG. 9 PRESSURE-EQUILIBRIUM PHASE COMPOSITION DIAGRAM FOR THE CARBONYL SULFIDE-PROPANE SYSTEM AT 60°F

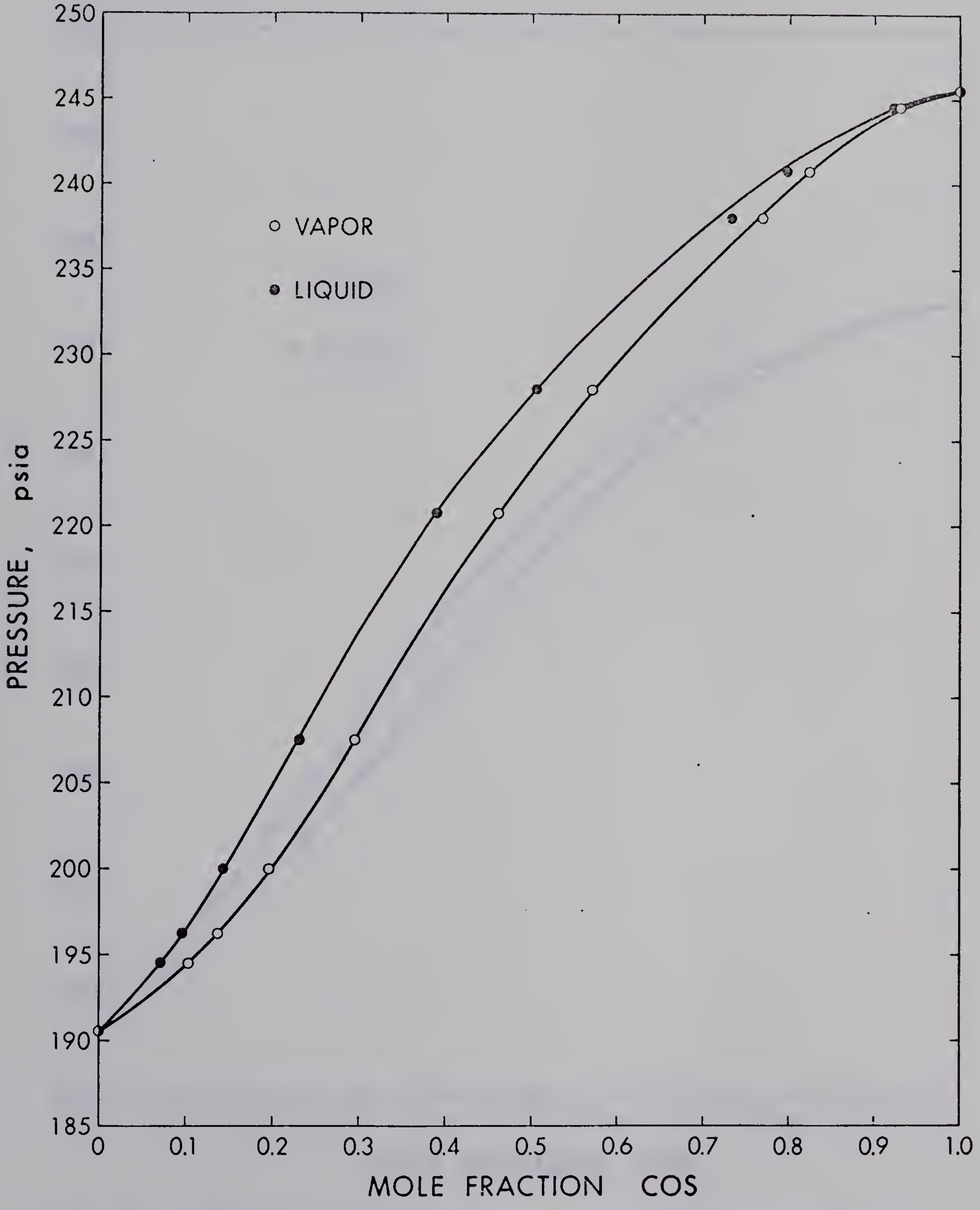

FIG. 10 PRESSURE-EQUILIBRIUM PHASE COMPOSITION DIAGRAM FOR THE CARBONYL SULFIDE-PROPANE SYSTEM AT 100°F

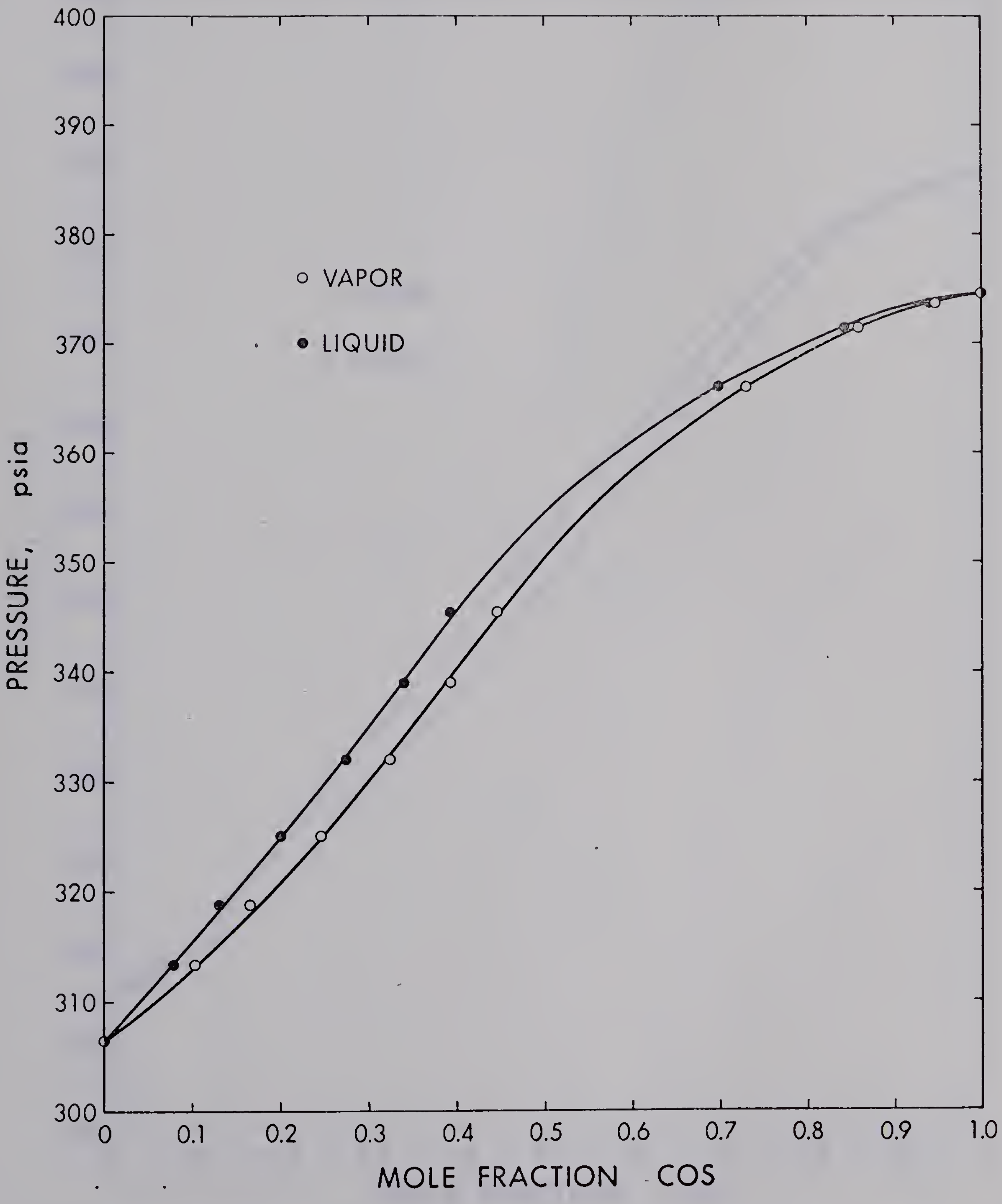

FIG. 11 PRESSURE-EQUILIBRIUM PHASE COMPOSITION DIAGRAM FOR THE CARBONYL SULFIDE-PROPANE SYSTEM AT 140°F

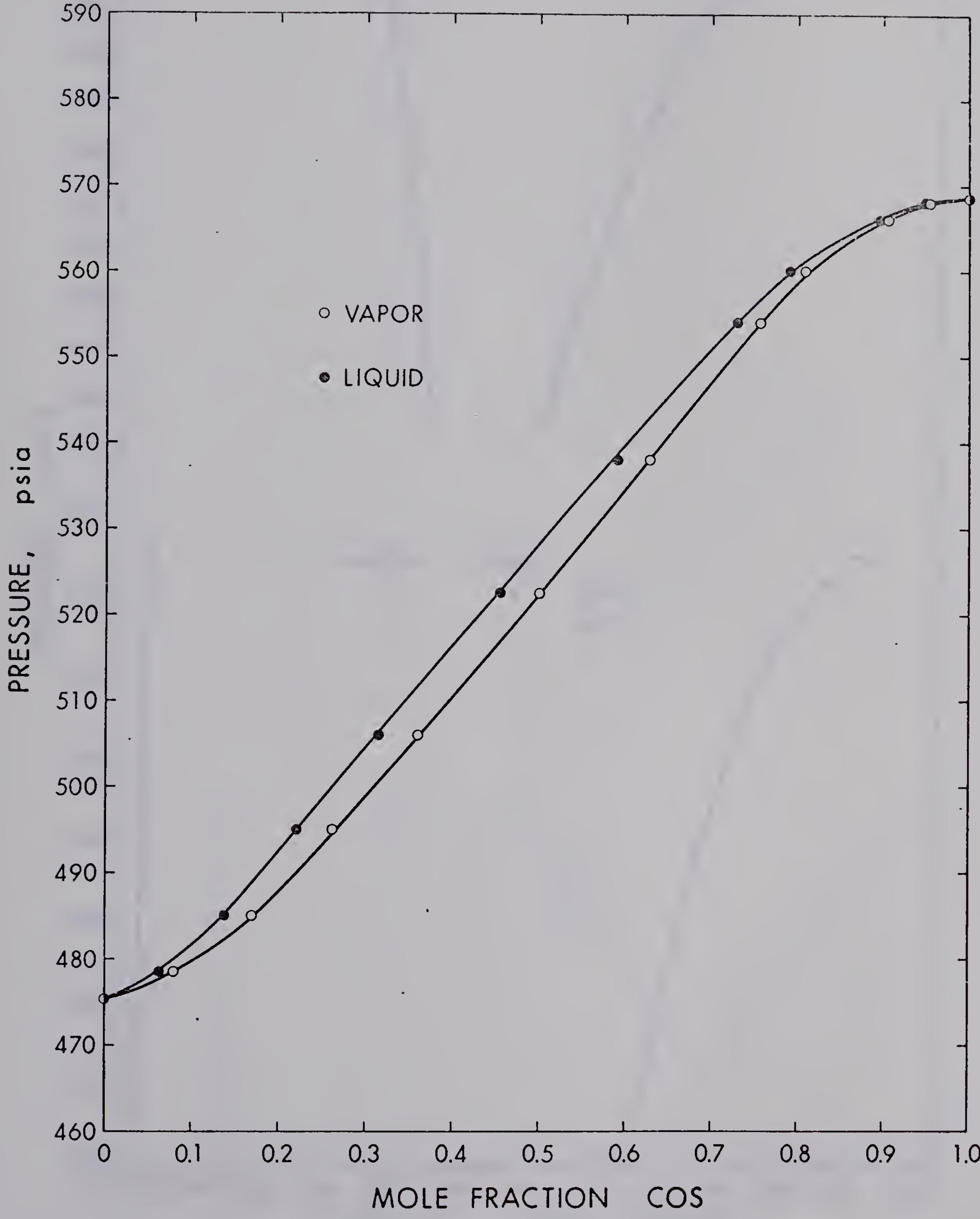

FIG. 12 PRESSURE-EQUILIBRIUM PHASE COMPOSITION DIAGRAM FOR THE CARBONYL SULFIDE-PROPANE SYSTEM AT 180°F

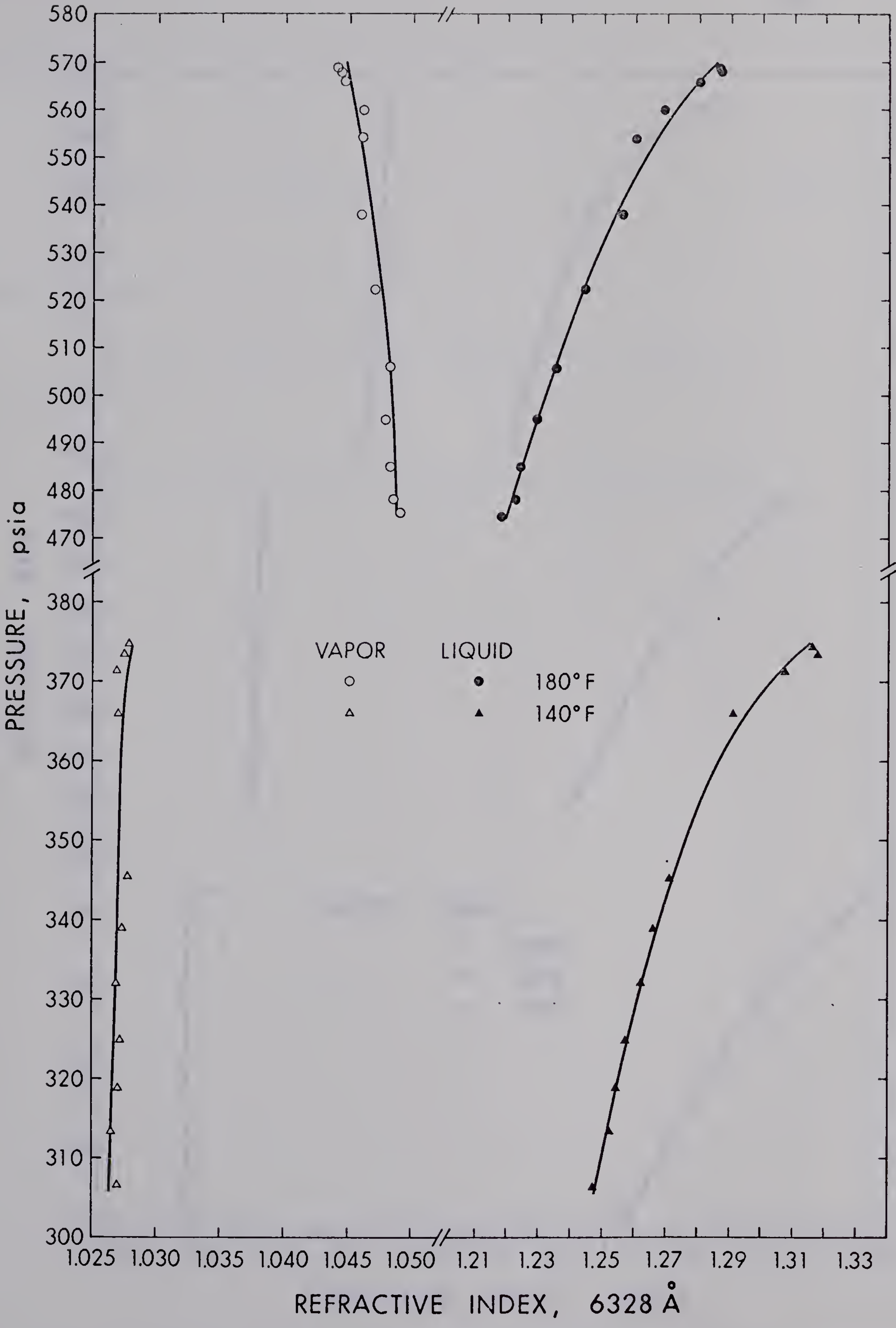

FIG. 13 PRESSURE-EQUILIBRIUM PHASE REFRACTIVE INDEX DIAGRAM FOR THE CARBONYL SULFIDE-PROPANE SYSTEM AT 140°F AND 180°F

[illegible]

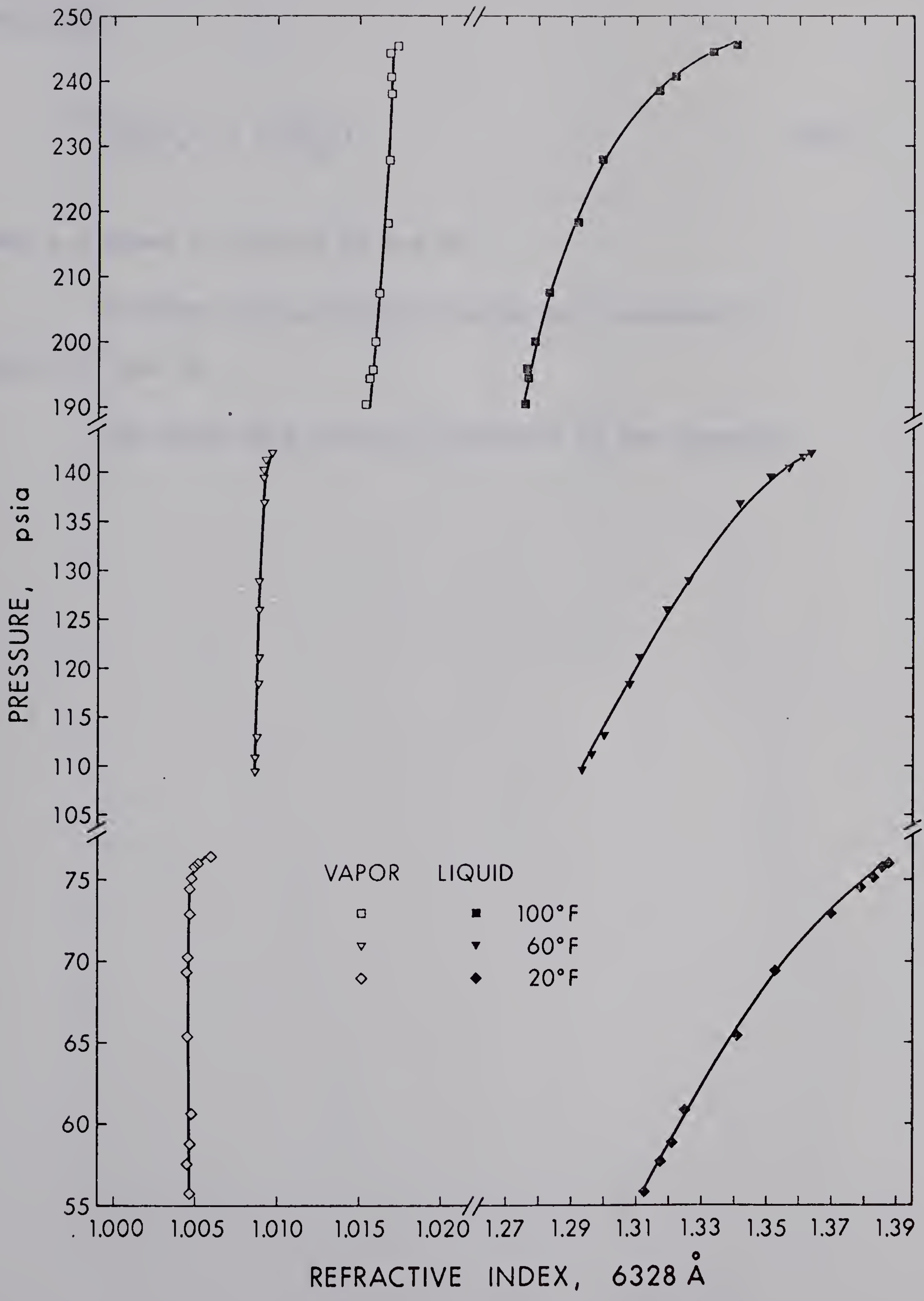

FIG. 14 PRESSURE-EQUILIBRIUM PHASE REFRACTIVE INDEX DIAGRAM FOR THE CARBONYL SULFIDE-PROPANE SYSTEM AT 20°F, 60°F AND 100°F

fractivity:

$$(R_{LL})_m = \sum x_i (R_{LL})_i \tag{20}$$

These are shown in Figures 15 and 16.

K-factor versus pressure curves are presented in Figures 17 and 18.

The above data are also tabulated in the Appendix.

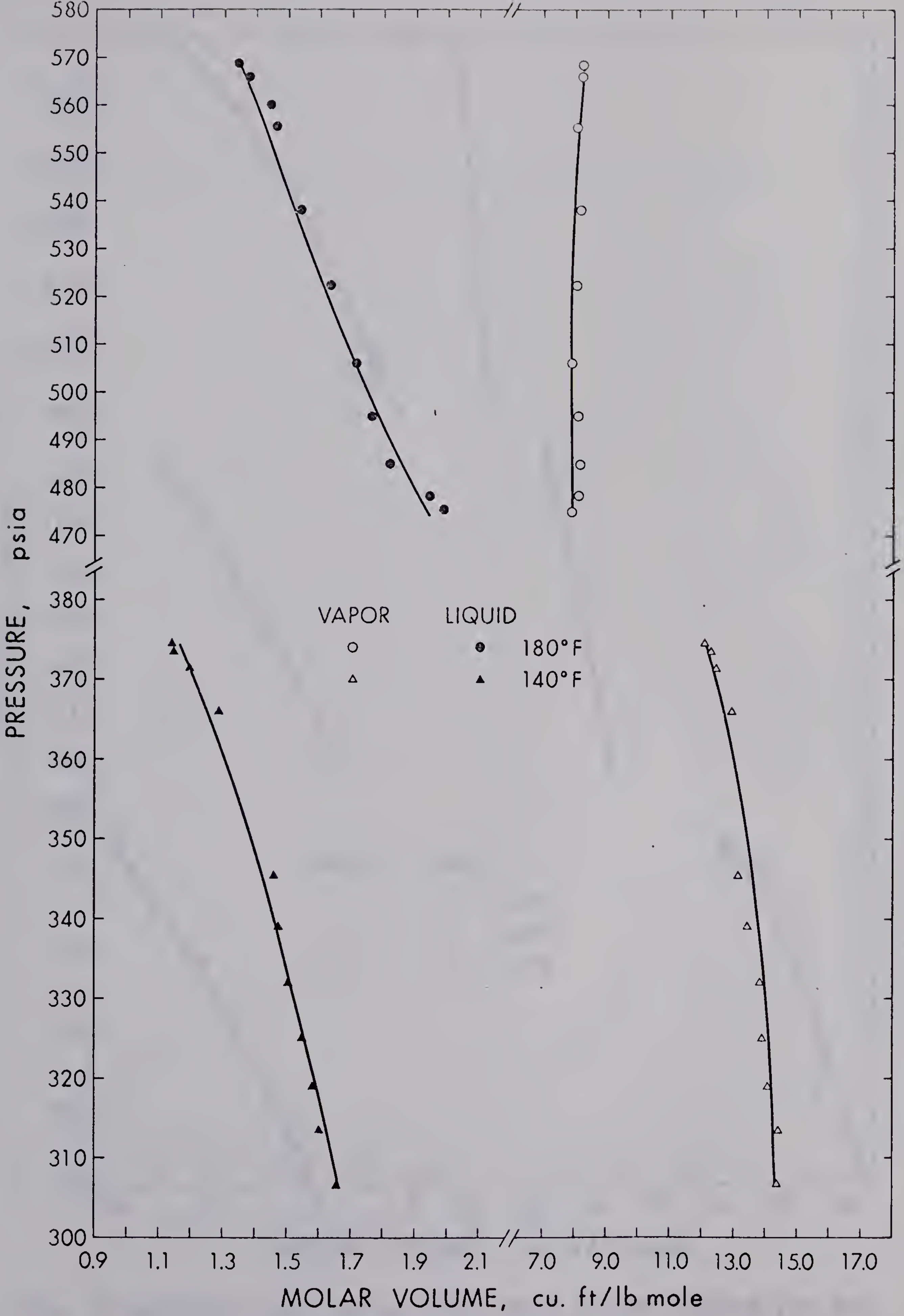

FIG. 15 PRESSURE-EQUILIBRIUM PHASE MOLAR VOLUME DIAGRAM FOR THE CARBONYL SULFIDE-PROPANE SYSTEM AT 140°F AND 180°F

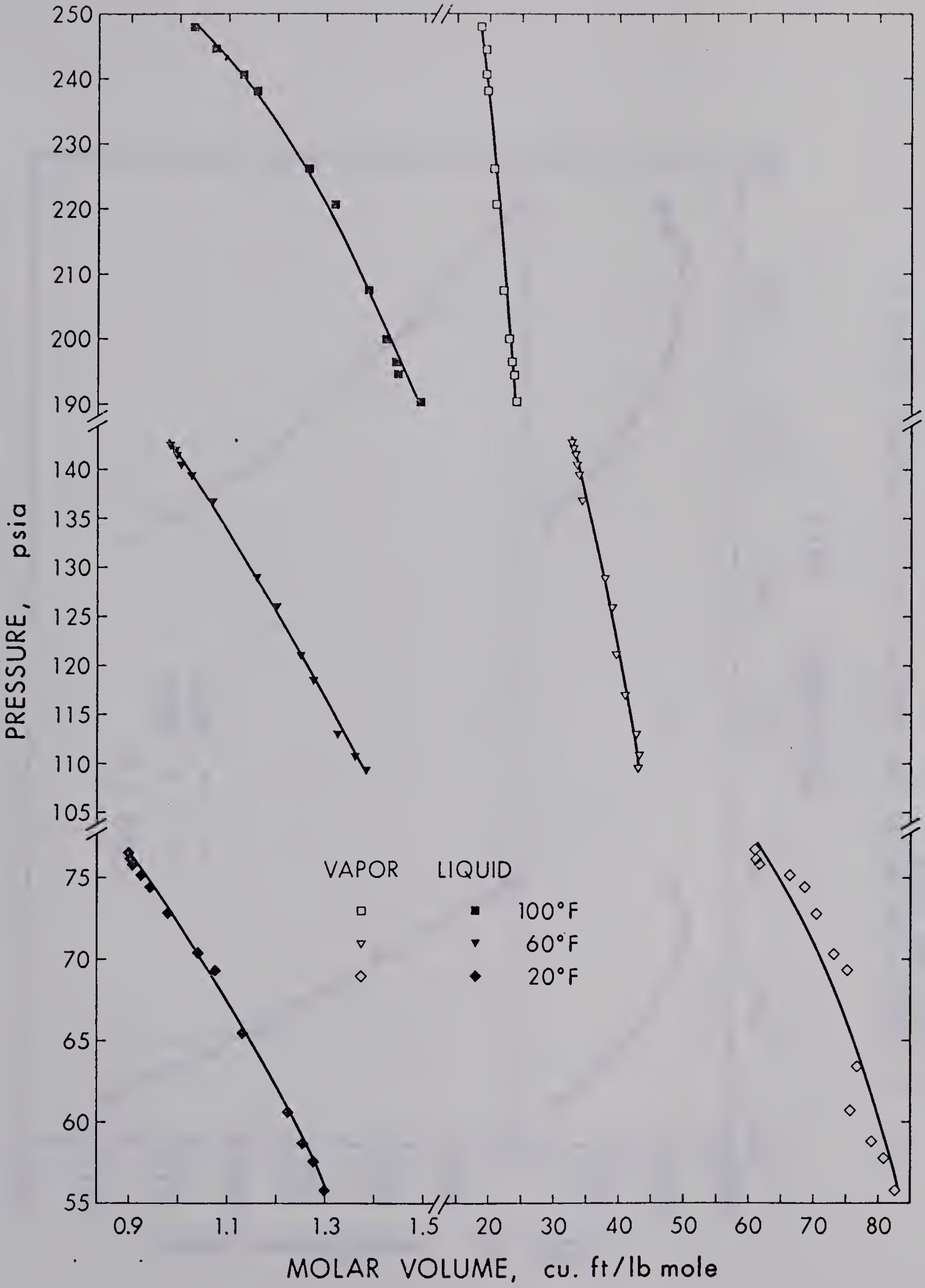

FIG. 16 PRESSURE-EQUILIBRIUM PHASE MOLAR VOLUME DIAGRAM FOR THE CARBONYL SULFIDE-PROPANE SYSTEM AT 20°F, 60°F AND 100°F

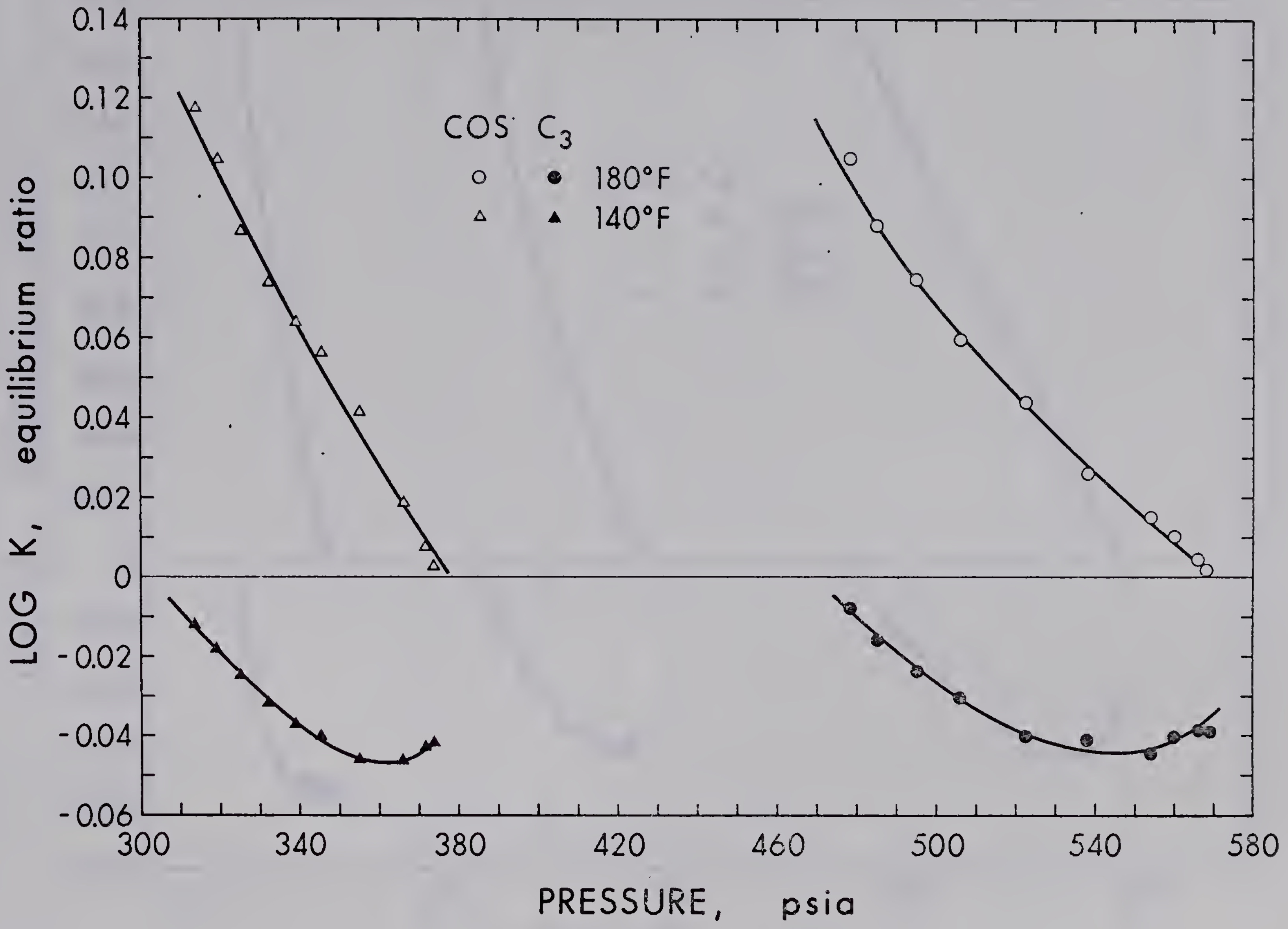

FIG. 17 EQUILIBRIUM RATIOS FOR CARBONYL SULFIDE-PROPANE SYSTEM AT 140°F AND 180°F

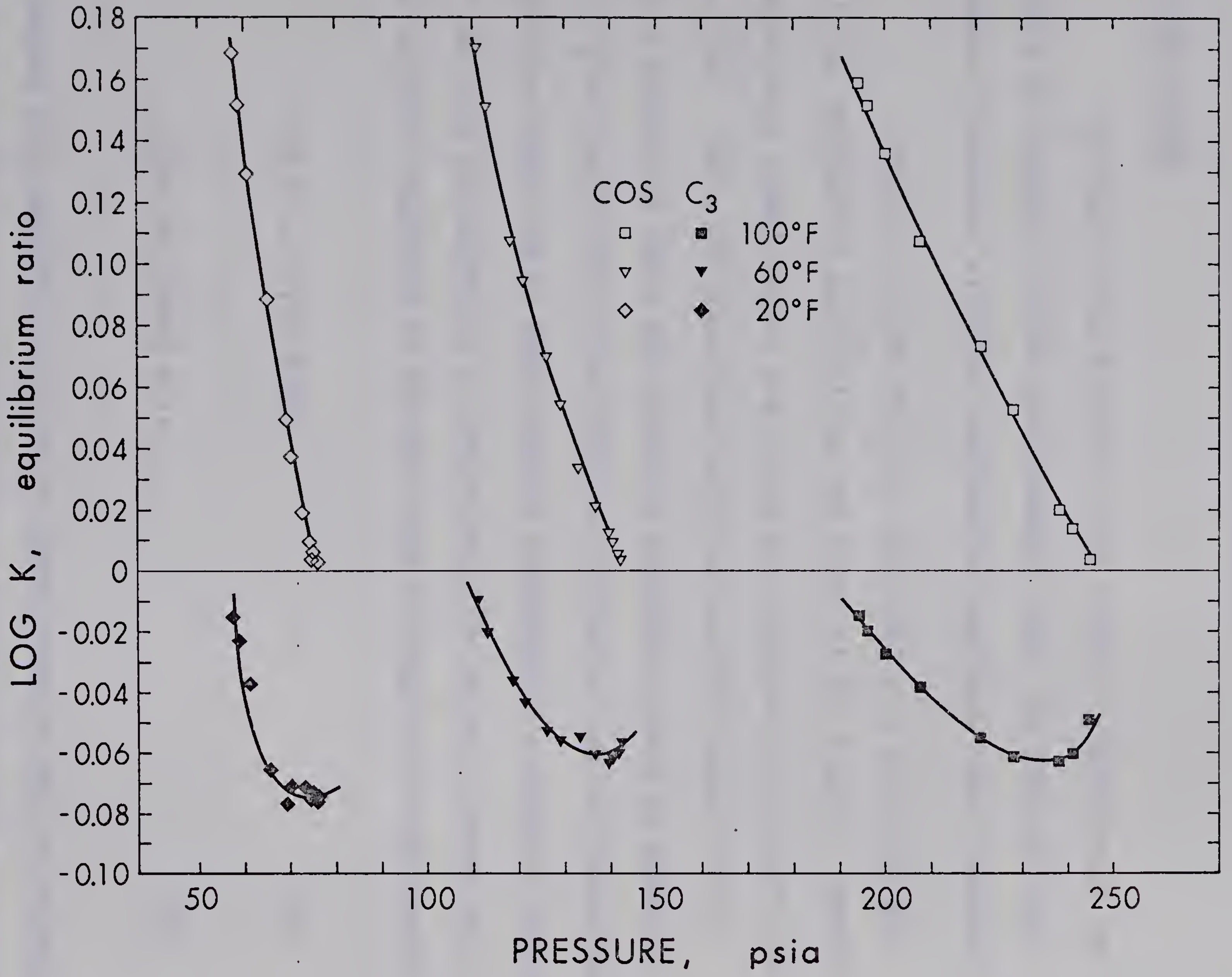

FIG. 18 EQUILIBRIUM RATIOS FOR CARBONYL SULFIDE-PROPANE SYSTEM AT 20°F, 60°F, AND 100°F

VI - DISCUSSION OF RESULTS

A) The System

In view of the fact that very little is known about the nature of carbonyl sulfide some comments about its physical and chemical behaviour with the experimental equipment seems relevant.

Carbonyl sulfide has been described as a colorless gas with no information available on the color of the liquid. However, during this investigation the liquid was observed to be bright red in color. One might speculate about the possible cause of this color wherein at least two plausible postulates could be examined. As a first possibility liquid COS may in fact be red or alternatively the color maybe due to some impurity generated by a chemical reaction of COS with the materials of construction of the equilibrium cell. Two possible reactions of COS with iron (Fe) may be written down as:

$$\mathrm{COS} + \mathrm{Fe} \rightarrow \mathrm{FeS} + \mathrm{CO}\uparrow \tag{21}$$

$$\mathrm{COS} + \mathrm{Fe} \rightarrow \mathrm{FeCO} + \mathrm{S}\downarrow \tag{22}$$

Equation (21) suggests evolution of carbon monoxide but no evidence of this was observed during vapor phase analysis on the gas chromatograph. Equation (22) appears to be the more plausible explanation since FeCO

is known to be red and a black solid deposit (possibly impure sulfur) was noticed on the inner surface of the equilibrium cell. More analytical work is however needed to confirm this hypothesis.

The red color mentioned above posed considerable difficulties in measuring the refractive index of the liquid phase mainly due to the fact that the laser light source used (6328 Å) was red in color and the ray of light transmitted through the liquid is to a great extent absorbed.

B) Determination of the Critical Point for Carbonyl Sulfide

The critical point was determined by plotting vapor pressures versus refractive indices of the saturated liquid and vapor phases. The critical temperature of COS was estimated by reading off the temperature corresponding to the critical pressure from a smoothed plot of the experimentally measured vapor pressure data versus temperature (Figure 7). The critical pressure and temperature obtained correspond to 960 psia and 235°F respectively.

Figure 19 shows a plot of the reduced pressure P_r versus the reduced temperature T_r of saturated COS. Experimental data are compared to a similar plot obtained from generalized tables of saturated fugacity coefficients as a function of P_r and T_r at different values of Z_c[79]. Excellent agreement is obtained between the generalized plot of Z_c=0.29 and the experimental values as indicated

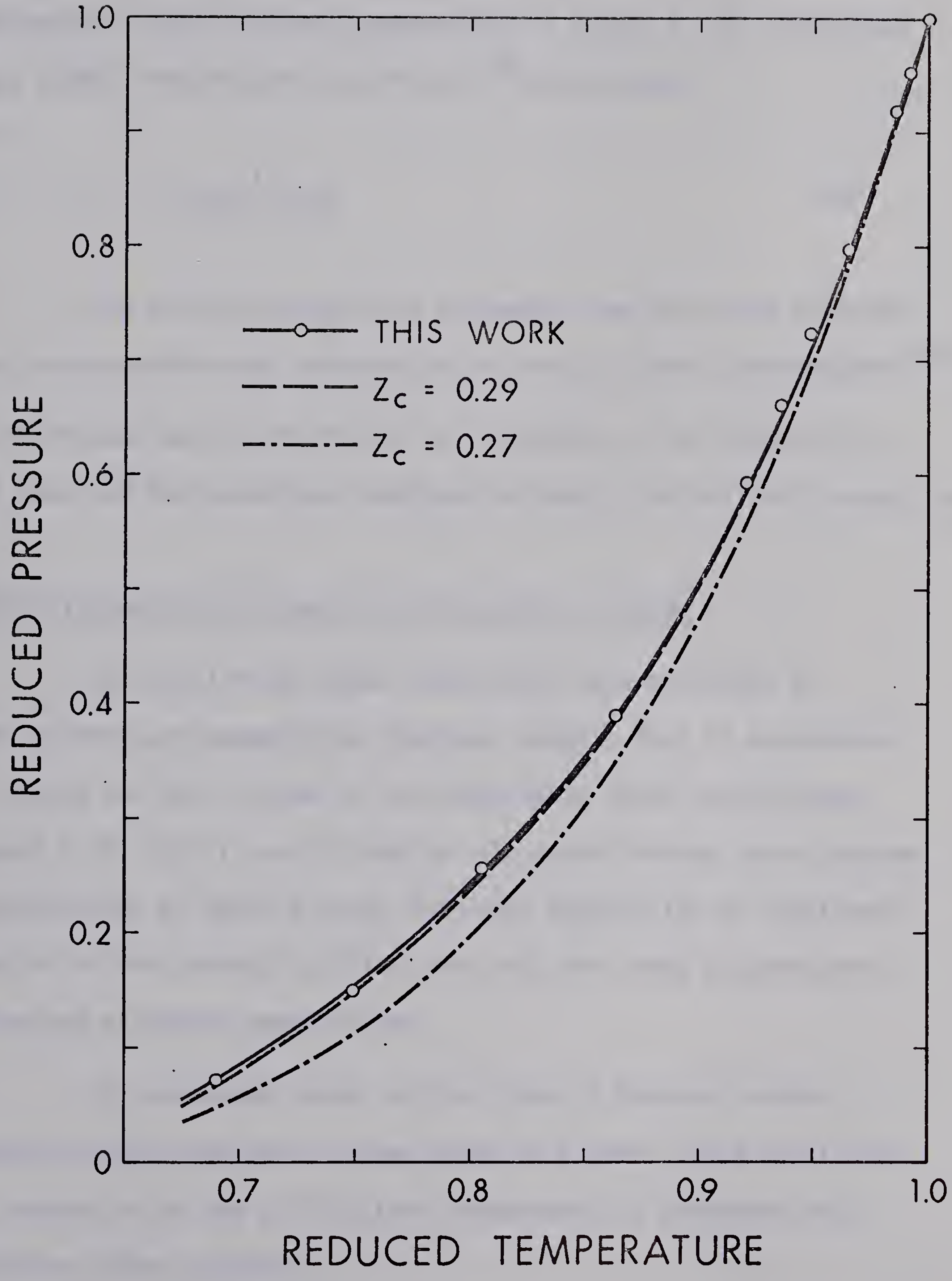

FIG. 19 REDUCED PRESSURE VS. REDUCED TEMPERATURE PLOT AT SATURATED CONDITIONS FOR CARBONYL SULFIDE

[illegible]

in Figure 19. The critical compresibility factor Z_c was calculated to be 0.287 from the Curl and Pitzer's[80] correlation:

$$Z_c = \frac{1}{1.28\omega + 3.41} \tag{23}$$

The critical properties estimated from this work indicate some discrepancies when compared to the work of other investigators[30,31,38,39]. The difference may be attributed to the purity of the COS used in each case and the techniques employed to obtain the critical properties.

C) Equilibrium Phase Properties of the COS-C_3 System

The equilibrium phase composition data obtained, as shown on pressure-composition diagrams, suggest that no azeotropes are formed for this system in the temperature range investigated. Figures 8, 9, 10, 11, and 12 show an elongated S-shape phase diagram. An examination of these figures indicates possibility of azeotropic behavior at the carbonyl sulfide rich end, the trend becoming more pronounced at higher temperatures.

The scattered points on the plots of pressure versus refractive index and molar volume shown in Figures 13,14 and 15,16 are indicative of the difficulties encountered in obtaining the refractive index readings.

Calculated equilibrium ratios based on the experimental

vapor-liquid equilibrium compositions are of a conventional shape when plotted with pressure. All of the isotherms exhibit a minimum value of K for the heavier component. These are shown in Figures 17 and 18.

VII - PREDICTION OF THE DATA AND THERMODYNAMIC CONSISTENCY TEST

General

A number of predictive methods are available for calculating multicomponent vapor-liquid equilibrium. Three of the more widely used are those of a) Chueh and Prausnitz[4] b) Benedict, Webb, and Rubin[25] and c) Soave-Redlich-Kwong[5]. Each of these is available in the form of a computer program. Basically each method utilizes the concept that $f_i^L = f_i^V$ at equilibrium. At a fixed temperature and liquid composition, the pressure and the vapor composition that satisfies the above condition are calculated. The Chueh-Prausnitz method was used exclusively for this investigation.

The modified version of the Chueh-Prausnitz phase behavior program called "CHUBIN" and the program called "FITTING" which estimates the value of the interaction constant α_{12} and the dilation constant η were used.

Chueh-Prausnitz Parameters

Owing to lack of binary data involving carbonyl sulfide with hydrocarbons, no information is available for a number of parameters needed in the "CHUBIN" and "FITTING" programs to predict the vapor-liquid equilibrium. Some of these parameters were estimated using the critical properties of the pure components and some were determined

by using the data obtained at 100°F. The constants were estimated so that the 100°F isotherm could be predicted. These constants were subsequently used to predict the phase behavior at the other temperatures. The estimated parameters are listed in Table 5.

Prediction of the Critical Properties of the Binary

The critical temperature, pressure, and molar volume of the binary, with mole fraction compositions incremented from 0.0 by 0.05 to 1.00 were predicted by the Chueh-Prausnitz computer program.

The predictions are tabulated in Table 7. The critical locus exhibited a minimum temperature of 194.1°F with a corresponding pressure of 559 psia.

Thermodynamic Consistency Test

The experimental data were tested for thermodynamic consistency by using a method presented by Chueh, Muirbrook, and Prausnitz[78]. The test was derived from the Gibbs-Duhem equation which for a binary system at constant temperature is:

$$x_1 d\ell n f_1 + x_2 d\ell n f_2 = v^L dP/RT$$

By appropriate thermodynamic substitution and mathematical manipulation, the authors show that a point by point consistency test can be arrived at as follows:

Area I + Area II + Area III =

$$[\ell n\ K_1 + \ell n\ \frac{\phi_1 P}{\phi_1{}^S P_1{}^S} + x_2(\ell n\ \frac{\phi_2}{\phi_1} + \ell n\ \frac{K_2}{K_1}\ )\ ]\ \text{at}\ x_2$$

where

$$\text{Area I} = \int_{x_2=0}^{x_2} \ell n\ \frac{K_2}{K_1}\ dx_2$$

$$\text{Area II} = \int_{x_2=0}^{x_2} \ell n\ \frac{\phi_2}{\phi_1}\ dx_2$$

$$\text{Area III} = \frac{1}{RT} \int_{x_2=0}^{x_2} v^L\ dP$$

The three areas were numerically integrated by using a method of assigned sample points at unequal intervals[81]. The fugacity coefficients, ϕ_i's were calculated from the Chueh-Prausnitz program, and the equilibrium ratios, K_i's were estimated from the experimental phase compositions.

Due to possible uncertainties in the evaluation of the fugacity coefficients through the use of an equation of state, the authors[78] judged that five per cent inconsistency constitutes a very good thermodynamic consistency test of the data.

Table 8 shows a comparison of the three areas, the left hand side and right hand side of the equation, and the percentage inconsistency for the five isotherms all calculated at x_2=1.0.

The test indicates an increasing inconsistency at elevated temperatures. This might be due to three possible reasons. Firstly,

the technique used in evaluating fugacity coefficients at high temperatures, especially near the critical region might contribute a significant error. Secondly, the possibility of large round off errors introduced by the nature of fugacity coefficients and the equilibrium ratios for each component are very close to each other which suggests that the ratio would be always close to unity. The natural logarithm of these ratios would be close to zero where small errors in the calculation would get magnified. Finally, the data itself could have some inconsistency.

VIII - SUMMARY AND CONCLUSIONS

The results and conclusions of the work undertaken and reported herein may be summarized as follows:

1. The equilibrium phase compositions and refractive indices have been measured for the carbonyl sulfide-propane binary system at 20°, 60°, 100°, 140°, and 180°F and at pressures between the vapor pressure of propane and carbonyl sulfide.

2. The refractive indices of pure carbonyl sulfide and pure propane were measured at each of the above temperatures to pressures of about 1000 psia.

3. The refractive indices of saturated liquid and saturated vapor carbonyl sulfide were measured at 11 temperatures between 20° and 230°F.

4. The vapor pressure of carbonyl sulfide has been measured from 20°F to 230°F.

5. The refractive index measurements and the vapor pressure and temperature measurements of the coexisting vapor and liquid phases for pure carbonyl sulfide have been used to estimate the following properties for carbonyl sulfide:

Critical Pressure	960 ± 5 psia
Critical Temperature	235 ± 1°F
Acentric Factor	0.056

The critical compressibility factor was calculated to be 0.287 and the critical volume was calculated to be 2.227 ft^3/lb-mole.

5. Numerical values have been obtained for the binary parameters required in using the Chueh-Prausnitz correlation for carbonyl sulfide-propane binaries, including k_{ij}, the deviation from the geometric mean for $T_{c_{ij}}$; τ_{ij} the parameter characteristic of the i-j interaction for T_c; ν_{ij}, the parameter characteristic of the i-j interaction for V_c; α_{ij}, the interaction parameter characteristic of the i-j interaction in the liquid solution at each of the experimental temperatures; and Ω_a and Ω_b for both liquid and vapor required in the Redlich-Kwong equation of state.

NOMENCLATURE

Å	Angstrom
C	Centigrade
F	Fahrenheit
G	Gibbs free energy
K	Vapor-liquid equilibrium constant
M	Molecular weight
P	Pressure
R	Universal gas constant
R_{LL}	Lorentz-Lorenz refractivity
S	Entropy
T	Temperature
U	Internal energy
V	Molar volume
Z	Compressibility factor
f	Fugacity
n	Refractive index
x	Mole fraction in the liquid
y	Mole fraction in the vapor

Greek letters

Ω_a, Ω_b	Redlich-Kwong constants

α	van Laar interaction parameter
β	Angle refraction of the window
$\mathscr{D}$	Correction for critical properties in the Chueh-Prausnitz computer program
γ	Activity coefficient
γ	Minimum deviation angle measured by autocollimation
δ	Prism angle
ρ	Density
ϕ	Fugacity coefficient
η	Dilation constant in the Chueh-Prausnitz program
τ	Parameter characteristic of the i-j interaction for T_C
ν	Parameter characteristic of the i-j interaction for V_C
μ	Chemical potential
ω	Acentric factor

Subscripts

C	Critical condition
E	Excess function
r	Reduced condition
i,j,k,etc.	Component identification
1,2	Component identification
ij	Interaction between i and j species

Superscripts

','',''',.	Denotes different phases
^	Denotes property in solution
L	Liquid
S	Saturated
V	Vapor

REFERENCES

[1] Pearce, R.L., Arnold, J.L., and Hall, C.K., Hydrocarbon Processing 40, (8), 121 (1961).

[2] Schulze, W.A., and Short, G.H., U.S. Patent 2,309,871 (February 2, 1943); Chem. Abstracts 37, 4559 (1943).

[3] Ferm, R.J., Chem. Review 57, 621 (1957).

[4] Prausnitz, J.M., and Chueh, P.L., Computer Calculations for High Pressure Vapor-Liquid Equilibria, Englewood Cliffs, N.J.: Prentice-Hall, Inc., 1968.

[5] Soave, G., Chem. Eng. Sci. 27, 1197 (1972).

[6] Sabra, A.I., Theories of Light from Descartes to Newton, New York, N.Y.: American Elsevier Publishing Co., Inc., 1967.

[7] Newton, I., Opticks, book II, 245 (1704)

[8] Laplace, P., Mec. Cel. 4, 32 (1806).

[9] Dulong, P., Ann. Chim. 31, (2), 154 (1826).

[10] Berthelot, M., Ann. Chim. 48, (3), 342 (1856).

[11] Gladstone, T., and Dale, T., Phil. Trans. 153, 317 (1863).

[12] Besserer, G.J., Ph.D. Thesis, University of Alberta, 1972.

[13] Lorentz, H., Wied. Ann. 9, 641 (1880).

[14] Lorenz, L., Wied. Ann. 11, 70 (1880).

[15] Batsanov, S.S., Refractometry and Chemical Structure, Trans. P.P. Sutton, New York: Consultants Bureau, 1961.

[16] Biot, I., and Arago, D., Mem. Inst. France 7, 301 (1806).

[17] Biot, I., and Arago, D., Ann. Phys. 25, 345 (1807).

[18] Smyth, C.P., Engel, E.W., and Wilson, Jr., E.G., J.A. C.S. 51, 1736 (1929).

[19] Young, J., and Finn, A., J. Research Nat. Bur. Stand. 25, 759 (1940).

[20] Keilich, S., Physica 28, 1116 (1962).

[21] Bloom, H., and Rhodes, A., J. Phys. Chem. 60, 791 (1956).

[22] Smith, J.M., and van Ness, H.C., Introduction to Chemical Engineering Thermodynamics, New York: McGraw-Hill Book Co., Inc., 1959.

[23] Chao, K.C., and Seader, J.D., A.I.Ch.E.J. 7 (4), 598 (1961).

[24] Benedict, M., Webb, G.B., and Rubin, L.C.,J.Chem.Phy. 8, 334 (1940).

[25] Benedict, M., Webb, G.B., and Rubin, L.C., Chem. Eng. Prog., 47 (8), 419 (1951).

[26] Opfell, J.B., and Sage, B.H., Ind. Eng. Chem., Chem.Eng. Data Ser., 1, 62 (1956).

[27] Pings, Jr., C.J., and Sage, B.H., Ind. Eng. Chem., Chem.Eng. Data Ser., 1, 56 (1956).

[28] Bishnoi, P.R., Miranda, R.D., and Robinson, D.B., "Improved BWR Coefficients", Hydrocarbon Processing, In Preparation.

[29] Than, C., Ann. Suppl. 5, 237 (1867).

[30] Ilosvay, M., Bull. Soc. Chim. 37, 294 (1882).

[31] Hempel, W., Z. angew. Chem. 14(92), 865 (1901).

[32] Stock, A., and Kuss, E., Ber. 50, 159 (1917).

[33] International Critical Tables, McGraw-Hill Publishing Company, Inc., New York, III, 231 (1928).

[34] Kemp, J.D., and Giauque, W.F., J.A.C.S. 59, 79 (1937).

[35] Honig, R.E., and Hook, H.O., R.C.A. Review 21, 360 (1960).

[36] Matheson Gas Products Company, 1973 Publication on COS.

[37] Pearson, T.G., Robinson, P.L., and Trotter, J., J. Chem. Soc. 660 (1932).

[38] Partington, J.R., and Neville, H.H., J. Phys. Colloid Chem. 55, 1550 (1951).

[39] Kobe, K.A., and Lynn, R.E., Jr., Chem. Review 52, 214 (1953).

[40] Lydersen, A.L. :Estimation of Critical Properties of Organic Compounds, Coll. Eng., Univ. Wisconsin, Eng. Expt. Sta. Rept. 3, Madison, Wis., April,1955.

[41] Francis, A.W., J. Chem. Eng. Data 5 (4), 534 (1960)

[42] Wong, L.Y., and Anderson, A., J. Optical Soc. Am. 62 (2), 219 (1972).

[43] Babb, Jr., S.E., J. Chem. Phys. 51, 847 (1969).

[44] Kir'yanova, T.V., and Pinsker, A.E., Khim. Prom. 43 (1), 30 (1967); Chem. Abstracts 66, 99011 (1967).

[45] Kobe, K.A., and Long, E.G., Petrol. Refiner 29 (1), 126 (1950).

[46] McBride, B.J., and Gordon, S., J. Chem. Phys. 35 (6), 2198 (1961).

[47] Zandler, M.E., Watson, Jr., J.A., and Eyring, H.J., Phys. Chem. 72 (8), 2730 (1968).

[48] Cross, P., J. Chem. Phys. 3, 825 (1935).

[49] Nelson, K.H., Veal, D., and Heinrich, B.J., Petrol. Ref. 34 (7), 155 (1955).

[50] Freise, F.W., Concrete Constr. Eng. 28, 299 (1933).

[51] Selleck, F.T., and Sage, B.H., A Comparison of Observed and Predicted Compressibility Factors for Propane, ADI Doc. 3914.

[52] Reamer, H.H., Sage, B.H., and Lacey, W.N., Ind. Eng. Chem. 41 (3), 482 (1949).

[53] Dittmar, P., Schulz, F., and Stresse, G., Chemie. Ing. Tech. 34, 437 (1962).

[54] Yesavage, V.F., Katz, D.L., and Powers, J.E., J. Chem. Eng. Data 14 (2), 197 (1969).

[55] Dana, L.I., Jenkins, A.C., Burdick, J.N., and Timm, R.C., Refrig. Eng. 12 (12), 387 (1926).

[56] Sage, B.H., Webster, D.C., and Lacey, W.N., Ind. Eng. Chem. 29 (11), 1309 (1937).

[57] Poettman, F.H., and Katz, D.L., Ind. Eng. Chem. 37 (9), 847 (1945).

[58] Price, A.R., and Kobayashi, R., J. Chem. Eng. Data 4 (1), 40 (1959).

[59] Kay, W.B., and Rambosek, G.M., Ind. Eng. Chem. 45 (1), 221 (1953).

[60] Sage, B.H., Lacey, W.N., and Schaafsma, J.G., Ind. Eng. Chem. 26 (2), 214 (1934).

[61] Reamer, H.H., Sage, B.H., and Lacey, W.N., Ind. Eng. Chem. 43 (1), 2512 (1951).

[62] Akers, W.W., Kelley, R.E., and Lipscomb, T.G., Ind. Eng. Chem. 46 (12), 2535 (1954).

[63] Brewer, J., Rodewald, N., and Kurata, F., A.I.Ch.E. J. 7 (1), 13 (1961).

[64] Reamer, H.H., Sage, B.H., and Lacey, W.N., Ind. Eng. Chem. 42 (3), 534 (1950).

[65] Sage, B.H., and Lacey, W.N., Ind. Eng. Chem. 32 (7), 992 (1940).

[66] Koonce, K.T., and Kobayashi, R., J. Chem. Eng. Data 9 (14), 494 (1964).

[67] Kay, W.B., and Rambosek, G.M., Ind. Eng. Chem. 45 (1), 221 (1953).

[68] Nysewander, C.N., Sage, B.H., and Lacey, W.N., Ind. Eng. Chem. 32 (1), 118 (1940).

[69] Gilliland, E.R., and Scheeline, H.W., Ind. Eng. Chem. 32 (1), 48 (1940).

[70] Akers, W.W., Burns, J.F., and Fairchild, W.R., Ind. Eng. Chem. 46 (12), 2531 (1954).

[71] Roof, J.G., and Baron, J.D., J. Chem. Eng. Data 12 (3), 292 (1967).

[72] Vairogs, J., Klekers, A.J., and Edmister, W.C., A.I.Ch.E. J. 17 (2), 308 (1971).

[73] Vaughan, W.E., and Collins, F.C., Ind. Eng. Chem. 34 (7), 885 (1942).

[74] Kay, W.B., J. Chem. Eng. Data 15 (1), 46 (1970).

[75] Djordjevich, L., and Budenholzer, R.A., J. Chem. Eng. Data 15 (1), 10 (1970).

[76] Besserer, G.J., and Robinson, D.B., Can. J. Chem. Eng. 49, 651 (1971).

[77] Robinson, D.B., and Besserer, G.J., Natural Gas Processors Association Research Report RR-7, June, 1972.

[78] Chueh, P.L., Muirbrook, N.K., and Prausnitz, J.M., A.I.Ch.E. J. 11 (6), 1097 (1965).

[79] Hougen, O.A., Watson, K.M., and Ragatz, R.A., Chemical Process Principles, Part II Thermodynamics, New York: John Wiley & Sons, Inc., 1959.

[80] Curl, R.F., and Pitzer, K.S., Ind. Eng. Chem. 50, 265 (1958).

[81] Hamming, R.W., Numerical Methods for Scientists and Engineers, Ch. 10, Toronto: McGraw Hill Book Co., 1962.

APPENDIX A

TABLE 1 : Effect of Temperature and Pressure on the Refractive Index of Carbonyl Sulfide

Pressure	Refractive Index*				
PSIA	20°F	60°F	100°F	140°F	180°F
76.5+	1.0062				
76.5++	1.3883				
113.0	1.3877				
142.5+		1.0098			
142.5++		1.3666			
213.5	1.3884	1.3672			
245.5+			1.0174		
245.5++			1.3412		
313.5	1.3891	1.3682	1.3424		
374.5+				1.0280	
374.5++				1.3151	
413.5	1.3894	1.3691	1.3438	1.3192	
513.5	1.3898	1.3698	1.3451	1.3209	
568.5+					1.0444
568.5++					1.2863
613.5	1.3904	1.3707	1.3464	1.3227	1.2881
713.5	1.3910	1.3715	1.3476	1.3246	1.2922
813.5	1.3916	1.3723	1.3487	1.3267	1.2953
913.5	1.3922	1.3732	1.3498	1.3284	1.2984
1013.5	1.3928	1.3739	1.3507	1.3299	1.3015

* Relative to vacuum at 6328 Å

\+ Saturated Vapor

++ Saturated Liquid

TABLE 2 : Effect of Temperature and Pressure on the Refractive Index Of Propane

Pressure	Refractive Index*				
PSIA	20°F	60°F	100°F	140°F	180°F
55.8[+]	1.0047				
55.8[++]	1.3128				
109.5[+]		1.0088			
109.5[++]		1.2938			
112.3	1.3133				
190.5[+]			1.0155		
190.5[++]			1.2722		
213.5	1.3142	1.2949	1.2727		
306.5[+]				1.0271	
306.5[++]				1.2465	
313.5	1.3148	1.2959	1.2744		
413.5	1.3156	1.2970	1.2757	1.2498	
475.5[+]					1.0491
475.5[++]					1.2101
513.5	1.3163	1.2980	1.2773	1.2525	1.2131
613.5	1.3170	1.2989	1.2787	1.2550	1.2206
713.5	1.3177	1.2996	1.2801	1.2572	1.2264
813.5	1.3183	1.3006	1.2814	1.2593	1.2308
913.5	1.3189	1.3015	1.2830	1.2613	1.2340
1013.5	1.3195	1.3023	1.2838	1.2631	1.2373

* Relative to vacuum at 6328 Å

[+] Saturated Vapor

[++] Saturated Liquid

TABLE 3 : Refractive Indices of Carbonyl Sulfide at Saturated Conditions

Pressure	Refractive Index*					
PSIA	20°F		60°F		77°F	
	Sat'd.Vapor	Sat'd.Liquid	Sat'd.Vapor	Sat'd.Liquid	Sat'd.Vapor	Sat'd.Liquid
76.5	1.0062	1.3883				
142.5			1.0098	1.3666		
183.0					1.0128	1.3528
	100°F		140°F		180°F	
	Sat'd.Vapor	Sat'd.Liquid	Sat'd.Vapor	Sat'd.Liquid	Sat'd.Vapor	Sat'd.Liquid
245.5	1.0174	1.3412				
374.5			1.0280	1.3151		
568.5					1.0444	1.2863
	190°F		200°F		210°F	
	Sat'd.Vapor	Sat'd.Liquid	Sat'd.Vapor	Sat'd.Liquid	Sat'd.Vapor	Sat'd.Liquid
635.5	1.0508	1.2733				
693.5			1.0574	1.2638		
766.5					1.0672	1.2543
	220°F		225°F		230°F	
	Sat'd.Vapor	Sat'd.Liquid	Sat'd.Vapor	Sat'd.Liquid	Sat'd.Vapor	Sat'd.Liquid
841.5	1.0776	1.2379				
881.5			1.0959	1.2229		
914.5					1.0997	1.1003

* Relative to vacuum at 6328 Å

TABLE 4 : Experimental Equilibrium Phase Properties for the Carbonyl Sulfide-Propane System

20°F

Pressure	Composition+		Refractive Index*		Molar Volume**		Equilibrium Constant	
PSIA	x	y	n_L	n_V	v_L	v_V	K_{COS}	K_{C3}
55.8	0.0000	0.0000	1.3128	1.0047	1.298	82.659	1.5650++	1.0000
57.6	0.0691	0.1019	1.3176	1.0046	1.276	80.707	1.4747	0.9648
58.8	0.1101	0.1562	1.3212	1.0047	1.253	78.693	1.4187	0.9482
60.8	0.1935	0.2605	1.3260	1.0048	1.221	75.688	1.3462	0.9169
65.4	0.3870	0.4743	1.3417	1.0045	1.130	76.715	1.2256	0.8576
69.3	0.5736	0.6431	1.3527	1.0045	1.063	75.167	1.1212	0.8370
70.3	0.6231	0.6799	1.3571	1.0046	1.039	73.086	1.0912	0.8493
72.9	0.7443	0.8089	1.3702	1.0047	0.980	70.498	1.0447	0.8467
74.6	0.8769	0.8966	1.3792	1.0047	0.941	68.693	1.0225	0.8399
75.1	0.9110	0.9250	1.3834	1.0049	0.925	66.348	1.0154	0.8427
75.8	0.9532	0.9607	1.3867	1.0052	0.911	61.557	1.0079	0.8397
76.0	0.9701	0.9748	1.3890	1.0052	0.904	61.306	1.0048	0.8428
76.5	1.0000	1.0000	1.3883	1.0062	0.901	60.010	1.0000	0.8550++

+ mole fraction COS

++ extrapolated

* relative to vacuum at 6328 Å

** ft^3/lb-mole calculated from the refractive index and composition data; Molar volume for pure C_3 was predicted by BWR equation with improved coefficients(28), and for pure COS, interpolated from the data of Partington and Neville(38).

TABLE 4 (Continued)

60°F

Pressure	Composition[+]		Refractive Index[*]		Molar Volume[**]		Equilibrium Constant	
PSIA	x	y	n_L	n_V	v_L	v_V	K_{COS}	K_{C3}
109.5	0.0000	0.0000	1.2938	1.0088	1.384	42.910	1.5400[++]	1.0000
110.8	0.0427	0.0632	1.2968	1.0087	1.357	43.297	1.4801	0.9786
113.0	0.1006	0.1426	1.3020	1.0087	1.324	42.616	1.4175	0.9533
118.4	0.2234	0.2862	1.3081	1.0089	1.276	40.880	1.2811	0.9191
121.2	0.2802	0.3485	1.3116	1.0091	1.249	39.612	1.2436	0.9051
126.0	0.3910	0.4600	1.3197	1.0091	1.201	39.062	1.1765	0.8867
129.0	0.4713	0.5342	1.3263	1.0093	1.161	37.814	1.1335	0.8810
136.8	0.7165	0.7531	1.3429	1.0098	1.068	34.342	1.0511	0.8709
139.4	0.8169	0.8414	1.3518	1.0094	1.026	33.901	1.0300	0.8662
140.4	0.8558	0.8747	1.3570	1.0094	0.998	33.603	1.0221	0.8689
141.6	0.9162	0.9270	1.3604	1.0094	0.988	33.211	1.0118	0.8711
142.0	0.9454	0.9521	1.3640	1.0094	0.973	33.016	1.0071	0.8773
142.5	1.0000	1.0000	1.3666	1.0098	0.960	32.601	1.0000	0.8950[++]

(see footnote on page 69)

TABLE 4 (Continuted)

		100°F						
Pressure	Composition$^+$		Refractive Index*		Molar Volume**		Equilibrium Constant	
PSIA	x	y	n_L	n_V	v_L	v_V	K_{COS}	K_{C3}
190.5	0.0000	0.0000	1.2722	1.0155	1.494	24.361	1.5300^{++}	1.0000
194.5	0.0715	0.1031	1.2778	1.0157	1.444	23.925	1.4420	0.9660
196.2	0.0969	0.1375	1.2763	1.0159	1.445	23.590	1.4190	0.9550
200.0	0.1436	0.1968	1.2791	1.0161	1.423	23.057	1.3705	0.9379
207.5	0.2300	0.2945	1.2832	1.0164	1.386	22.366	1.2804	0.9162
220.8	0.3899	0.4620	1.2925	1.0168	1.313	21.300	1.1849	0.8818
228.0	0.5056	0.5706	1.2994	1.0169	1.263	20.735	1.1286	0.8685
238.0	0.7325	0.7685	1.3171	1.0171	1.317	19.879	1.0491	0.8654
240.8	0.7972	0.8231	1.3221	1.0170	1.127	19.837	1.0325	0.8723
244.5	0.9222	0.9305	1.3340	1.0168	1.068	19.659	1.0090	0.8933
245.5	1.0000	1.0000	1.3412	1.0174	1.035	18.812	1.0000	0.9200^{++}

(See footnote on page 69)

TABLE 4 (Continued)

140°F

Pressure	Composition[+]		Refractive Index[*]		Molar Volume[**]		Equilibrium Constant	
PSIA	x	y	n_L	n_V	v_L	v_V	K_{COS}	K_{C3}
306.5	0.0000	0.0000	1.2465	1.0271	1.657	14.372	1.3760[++]	1.0000
313.5	0.0784	0.1027	1.2522	1.0265	1.604	14.456	1.3099	0.9736
319.0	0.1302	0.1657	1.2541	1.0270	1.582	14.088	1.2726	0.9592
325.0	0.2000	0.2442	1.2651	1.0271	1.549	13.907	1.2210	0.9448
332.0	0.2731	0.3239	1.2621	1.0269	1.508	13.856	1.1860	0.9301
339.0	0.3390	0.3930	1.2653	1.0274	1.476	13.465	1.1593	0.9183
345.5	0.3920	0.6080	1.2661	1.0278	1.465	13.166	1.1383	0.9108
366.0	0.6991	0.7297	1.2923	1.0271	1.283	12.953	1.0438	0.8983
371.5	0.8434	0.8580	1.3077	1.0276	1.198	12.474	1.0173	0.9068
373.6	0.9413	0.9467	1.3182	1.0261	1.145	12.320	1.0057	0.9080
374.5	1.0000	1.0000	1.3151	1.0280	1.147	12.067	1.0000	0.9250[++]

(See footnote on page 69)

TABLE 4 (Continued)

180°F

Pressure	Composition$^+$		Refractive Index*		Molar Volume**		Equilibrium Constant	
PSIA	x	y	n_L	n_V	v_L	v_V	K_{COS}	K_{C3}
475.4	0.0000	0.0000	1.2101	1.0491	1.991	7.937	1.3150^{++}	1.0000
478.5	0.0630	0.0802	1.2226	1.0490	1.845	8.134	1.2730	0.9816
485.0	0.1386	0.1697	1.2240	1.0481	1.821	8.139	1.2244	0.9639
495.0	0.2212	0.2626	1.2292	1.0480	1.768	8.100	1.1872	0.9468
506.0	0.3141	0.3605	1.2352	1.0487	1.713	7.912	1.1477	0.9324
522.5	0.4541	0.5025	1.2443	1.0472	1.633	8.057	1.1066	0.9113
538.0	0.5922	0.6289	1.2563	1.0461	1.542	8.149	1.0620	0.9100
554.0	0.7295	0.7560	1.2601	1.0462	1.461	8.048	1.0363	0.9020
560.0	0.7900	0.8087	1.2693	1.0464	1.447	7.969	1.0238	0.9110
566.0	0.8960	0.9050	1.2805	1.0447	1.380	8.207	1.0100	0.9135
568.0	0.9493	0.9537	1.2871	1.0444	1.345	8.211	1.0046	0.9132
568.5	1.0000	1.0000	1.2863	1.0444	1.345	8.181	1.0000	0.9400^{++}

(See footnote on page 69)

APPENDIX B

TABLE 5 : Chueh-Prausnitz Parameters for the Pure COS and C_3 and its Binary

$\omega_{COS} = 0.056$

$\omega_{C_3} = 0.152$

$\tau_{12} = -48.71°R$

$\nu_{12} = -0.353 ft^3/lb\text{-}mole$

$k_{ij} = 0.0044$

$\Omega_{a_V} = 0.33$

$\Omega_{a_L} = 0.49$

$\Omega_{b_V} = 0.075$

$\Omega_{b_L} = 0.098$

Temperature (°F)	α_{12} (lb-mole/cu.ft.)
20	0.0363
60	0.0470
100	0.0460
140	0.0335
180	0.0151

TABLE 6 : Comparison of the Chueh-Prausnitz Predictions and Experimental Equilibrium Ratio, K

20°F

Pressure		Carbonyl Sulfide			Propane		
PSIA	x_{cos}	$K_{exp.}$	K_{C-P}	% Dev.*	$K_{exp.}$	K_{C-p}	% Dev.*
57.6	0.0691	1.4748	1.4228	-3.5	0.9648	0.9687	0.4
58.8	0.1101	1.4187	1.3903	-2.0	0.9482	0.9518	0.4
60.8	0.1935	1.3462	1.3296	-1.2	0.9169	0.9210	0.4
65.4	0.3870	1.2256	1.2125	-1.1	0.8576	0.8659	1.0
69.3	0.5736	1.1211	1.1250	0.3	0.8370	0.8320	-0.6
70.3	0.6231	1.0912	1.1053	1.3	0.8493	0.8259	-2.8
72.9	0.7743	1.0447	1.0538	0.9	0.8467	0.8155	-3.7
75.6	0.8769	1.0225	1.0259	0.3	0.8400	0.8158	-2.9
75.1	0.9110	1.0154	1.0179	0.2	0.8427	0.8173	-3.0
75.8	0.9532	1.0079	1.0088	0.1	0.8397	0.8204	-2.3
76.0	0.9701	100.48	1.0055	0.1	0.8428	0.8219	-2.5

* With respect to experimental value

TABLE 6 (Continued)

60°F

Pressure			Carbonyl	Sulfide		Propane	
PSIA	x_{cos}	$K_{exp.}$	K_{C-P}	%Dev.*	$K_{exp.}$	K_{C-P}	% Dev.*
110.8	0.0427	1.4801	1.4463	-2.3	0.9786	0.9801	0.2
113.0	0.1006	1.4175	1.3960	-1.5	0.9533	0.9558	0.3
118.4	0.2234	1.2811	1.3030	1.7	0.9191	0.9129	-0.7
121.2	0.2802	1.2438	1.2655	1.7	0.9051	0.8967	-0.9
126.0	0.3910	1.1765	1.2007	2.1	0.8867	0.8712	-1.7
129.0	0.4713	1.1335	1.1600	2.3	0.8810	0.8574	-2.7
136.8	0.7165	1.0511	1.0635	1.2	0.8709	0.8397	-3.6
139.4	0.8169	1.0300	1.0350	0.5	0.8662	0.8438	-2.6
140.4	0.8558	1.0221	1.0257	0.4	0.8689	0.8474	-2.5
141.6	0.9162	1.0188	1.0133	0.1	0.8711	0.8557	-1.8
142.0	0.9454	1.0071	1.0081	0.1	0.8773	0.8608	-1.9

* With respect to experimental value

TABLE 6 (Continued)

100°F

Pressure			Carbonyl Sulfide			Propane	
PSIA	x_{cos}	$K_{exp.}$	K_{C-P}	% Dev*	$K_{exp.}$	K_{C-P}	% Dev.*
194.5	0.0715	1.4420	1.3526	-6.2	0.9660	0.9729	0.7
196.2	0.0969	1.4190	1.3345	-6.0	0.9550	0.9642	1.0
200.0	0.1436	1.3705	1.3030	-4.9	0.9379	0.9493	1.2
207.5	0.2300	1.2804	1.2500	-2.4	0.9162	0.9254	1.0
220.8	0.3899	1.1849	1.1677	-1.5	0.8818	0.8929	1.3
228.0	0.5056	1.1286	1.1191	-0.8	0.8685	0.8782	1.1
238.0	0.7325	1.0491	1.0470	-0.2	0.8654	0.8717	0.7
240.8	0.7972	1.0325	1.0317	-0.1	0.8723	0.8758	0.4
244.5	0.9222	1.0090	1.0091	0.0	0.8933	0.8929	-0.1

* With respect to experimental value

TABLE 6 (Continued)

140°F

Pressure			Carbonyl Sulfide			Propane	
PSIA	x_{cos}	$K_{exp.}$	K_{C-P}	% Dev.*	$K_{exp.}$	K_{C-p}	% Dev.*
313.5	0.0784	1.3099	1.2515	-4.5	0.9736	0.9786	0.5
319.0	0.1302	1.2726	1.2278	-3.5	0.9592	0.9660	0.7
325.0	0.2000	1.2210	1.1980	-1.9	0.9448	0.9506	0.6
332.0	0.2731	1.1860	1.1694	-1.4	0.9301	0.9364	0.7
339.0	0.3390	1.1593	1.1454	-1.2	0.9183	0.9254	0.8
345.5	0.3920	1.1383	1.1278	-0.9	0.9108	0.9177	0.7
366.0	0.6991	1.0438	1.0459	0.2	0.8983	0.8936	-0.5
371.5	0.8434	1.0173	1.0193	0.2	0.9068	0.8963	-1.2
373.6	0.9413	1.0057	1.0060	0.0	0.9080	0.9044	-0.4

* With respect to experimental value

TABLE 6 (Continued)

		180°F					
Pressure			Carbonyl Sulfide			Propane	
PSIA	x_{cos}	$K_{exp.}$	K_{C-P}	% Dev.*	$K_{exp.}$	K_{C-P}	% Dev.*
478.5	0.0630	1.2730	1.1157	-12.4	0.9816	0.9923	1.1
485.0	0.1386	1.2244	1.1119	- 9.2	0.9639	0.9821	1.9
495.0	0.2212	1.1872	1.1044	- 7.0	0.9468	0.9705	2.5
506.0	0.3141	1.1477	1.0935	- 4.7	0.9324	0.9573	2.7
522.5	0.4541	1.1066	1.0744	- 2.9	0.9113	0.9382	2.9
538.0	0.5922	1.0620	1.0545	- 0.7	0.9100	0.9210	1.2
554.0	0.7295	1.0363	1.0348	- 0.1	0.9020	0.9065	0.5
560.0	0.7900	1.0237	1.0264	0.3	0.9110	0.9011	-1.1
566.0	0.8960	1.0100	1.0125	0.2	0.9135	0.8934	-2.2
568.0	0.9493	1.0046	1.0059	0.1	0.9132	0.8905	-2.5

* With respect to experimental value

TABLE 7 : Prediction of the Critical Properties of the Carbonyl Sulfide-Propane Binary

Composition x_{cos}	Temperature °F	Pressure PSIA	Molar Volume ft^3/lb-mole
0.0	206.20	618.7	3.180
0.0500	203.60	606.3	3.116
0.1000	201.28	594.8	3.052
0.1500	199.24	584.4	2.990
0.2000	197.51	575.4	2.928
0.2500	196.11	568.0	2.869
0.3000	195.06	562.7	2.810
0.3500	194.39	559.6	2.753
0.4000	194.12	559.4	2.698
0.4500	194.29	562.3	2.645
0.5000	194.91	568.9	2.594
0.5500	196.03	579.7	2.546
0.6000	197.69	595.2	2.499
0.6500	199.90	616.1	2.456
0.7000	202.73	642.9	2.415
0.7500	206.20	676.2	2.378
0.8000	210.36	716.7	2.344
0.8500	215.27	764.8	2.314
0.9000	220.97	821.2	2.288
0.9500	227.53	886.2	2.267
1.0000	235.00	960.0	2.250

TABLE 8 :Thermodynamic Consistency Test of the Data*

Isotherm °F	Area I	Area II	Area III	LHS	$\ell n\ K_1$	$\ell n\ \frac{\phi_1 P}{\phi_1^s P_1^s}$	$x_2(\ell n\ \frac{K_2}{K_1} + \ell n\ \frac{\phi_2}{\phi_1})$	RHS	% Inconsistency
20	0.3039	0.0459	0.0046	0.3544	-0.1567	0.2879	0.2034	0.3346	5.7
60	0.2568	0.0762	0.0072	0.3402	-0.1109	0.2297	0.1847	0.3035	11.4
100	0.2607	0.1096	0.0120	0.3823	-0.0834	0.2148	0.1921	0.3236	16.6
140	0.1973	0.1489	0.0153	0.3615	-0.0780	0.1779	0.2080	0.3079	16.0
180	0.1770	0.2000	0.0217	0.3987	-0.0619	0.1458	0.2334	0.3173	22.7

* COS(2) - C_3(1)

APPENDIX C

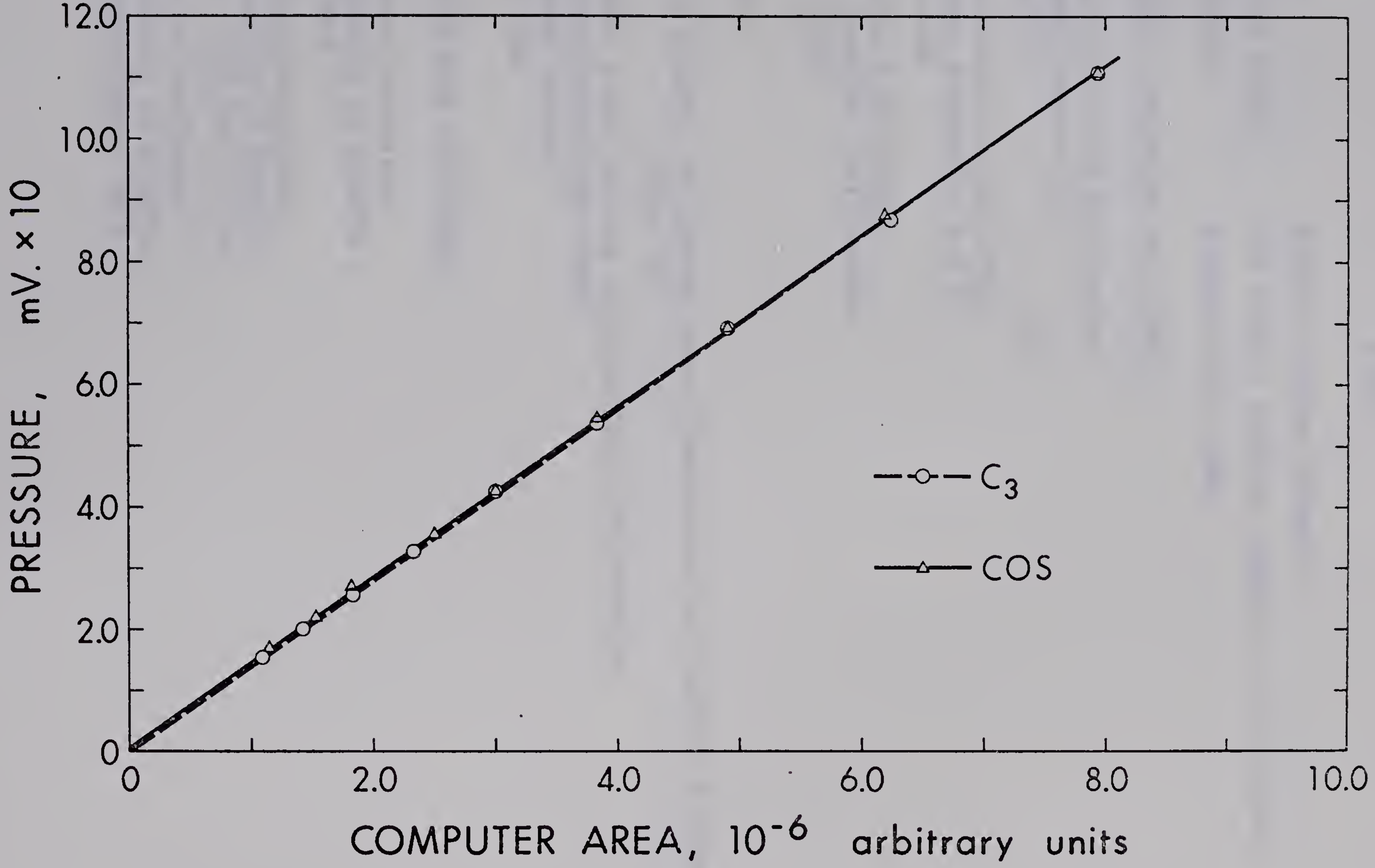

FIG. 20 GAS CHROMATOGRAPH CALIBRATION FOR CARBONYL SULFIDE-PROPANE